Journal of
Materials Chemistry C

Materials for optical, magnetic and electronic devices

Accepted Manuscript

This article can be cited before page numbers have been issued, to do this please use: S. Park, D. Chandrashekhar, N. Gan and F. Aniés, *J. Mater. Chem. C*, 2026, DOI: 10.1039/D6TC00010J.

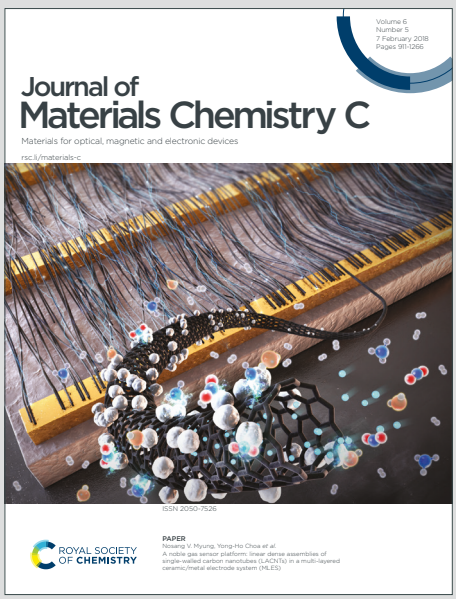

ROYAL SOCIETY OF CHEMISTRY

rsc.li/materials-c

View Article Online
DOI: 10.1039/D6TC00010J

HIGHLIGHT

Functional Organic Room-Temperature Phosphorescent Materials

Durga Chandrashekhar,[†a] Nan Gan,[†a] Filip Aniés[a] and So Min Park[*a]

Received 00th January 20xx,
Accepted 00th January 20xx

DOI: 10.1039/x0xx00000x

Organic room-temperature phosphorescence (RTP) materials are increasingly appearing in the research landscape for their comparative advantages over their conventional inorganic counterparts, such as synthetic simplicity and lower toxicity. However, emerging applications are driving a demand for additional functionalities in RTP materials. As a result, recent research has exhibited the benefits of introducing intrinsic functions, such as flexibility, and transductive functions, such as x-ray scintillation, as a response to the augmenting need to apply RTP materials within various fields. This review examines the recent progress of four such "functional" organic RTP materials: flexibile and stretchable; dynamic (e.g. mechanochromic); x-ray scintillating; and circularly polarizing. We discuss their properties and design strategies, studying recently reported literature, and discuss their great potential to emerging real-world applications. While independent reviews on some of these functions have been reported, this article comprehensively examines the current state of research into this prominent material class, taking a more mechanism-forward approach. In addition, this article discusses future research directions that can mitigate the challenges associated with these materials. We find that, within the scope of organic RTP materials, polymeric materials may be the most facile strategy to achieve much of these properties and encourage applicability, albeit all organic materials still requiring further optimization to ensure that functionalization does not come at the cost of efficient RTP.

1. Introduction

Materials exhibiting room-temperature phosphorescence (RTP) possess distinct properties such as large Stokes shifts and long-lived triplet excitons.[1,2] Moreover, RTP materials exhibit afterglow effects that are intuitive and observable by the naked eye.[3] These properties favour the use of such materials for a vast range of applications from optoelectronic devices and flexible displays to biological imaging and sensing, to phototherapy and information encryption.[4–6] In addition, when compared with steady-state luminescence spectroscopy, afterglow spectroscopy – such as that relying on RTP – can drastically increase the signal-to-noise ratios using time-resolved techniques.[3] Moreover, in comparison to their inorganic antecedents, purely organic RTP materials offer facile synthesis, lower toxicity, and greater applicability. Thus, these unique properties have generated a surge in research interest on organic RTP materials over the past 10 years or so (Figure 1).

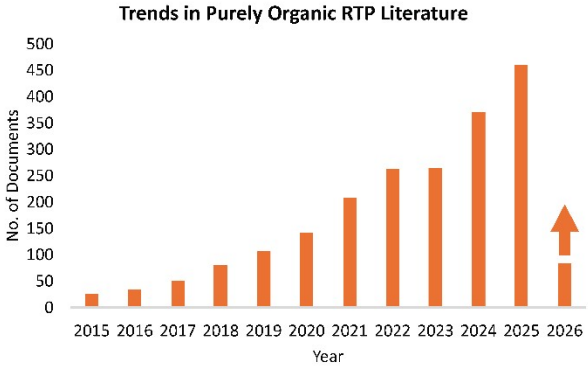

Fig. 1: Trends in purely organic RTP materials being reported in publications (based on Scopus database for a title, abstract, keyword analysis of (organic AND room AND temperature AND phosphorescence) AND NOT (metal AND complexes)).

RTP is a phosphorescence phenomenon which involves the spin-forbidden electronic transition via inter-system crossing (ISC) between the singlet and triplet states at ambient conditions. It was previously associated exclusively with metallic or inorganic complexes.[7] Since ISC and phosphorescence lifetime (τ_p) are highly dependent on efficient spin-orbit coupling (SOC), and oxygen, heat, and moisture are known to quench triplet excited states, purely organic molecules were originally believed to require cryogenic or inert conditions to exhibit phosphorescence.[7–9] However, precise molecular design and synthetic methods to combat these limitations has led to the realization of RTP in pure organic systems.[7,10] For instance, structures like difluoroboron

[a] Department of Chemistry, National University of Singapore, Singapore, 117543 Singapore
*Corresponding Author. Email: sompark@nus.edu.sg
†These authors contributed equally to this work.

dibenzoylmethane with polylactic acid (PLA) were observed to exhibit oxygen-sensitive RTP as early as 2007.[11] Additionally, these purely organic RTP materials surpass their inorganic/metallic predecessors owing to their lowered costs and toxicities.[12]

Figure 2 exhibits a common Jablonski diagram with the various transitions possible between electronic states. Upon absorption of a photon, electrons in the singlet ground state (S_0) are excited to excited singlet states (S_n) to form excitons that can undergo vibrational relaxations within the singlet excited state or drop down to the first excited singlet state (S_1) via an internal conversion (IC). From there, should the exciton drop directly to S_0 – a spin-allowed transition – the molecule would emit fluorescence. Alternatively, the exciton can undergo ISC to an excited triplet state (T_n). Further IC can occur to transition to the lowest stable triplet excited state (T_1) such that the exciton can, via radiative decay, transition back to S_0 through phosphorescence.

However, these singlet-triplet transitions are spin-forbidden, leading to τ_p being very long (micro to millisecond range or longer). Moreover, there is also a high probability of non-radiative decay.[1] Thus, efficient RTP materials, i.e., those with promising phosphorescent quantum yields (ϕ_p) and long τ_p, fulfil three major requirements: (1) spin-flipping via ISC from S_1 to T_n, (2) elimination of non-radiative relaxations or a reduced rate of non-radiative decay (k_{ISC}'), and (3) low phosphorescent rate (k_p).[10,13]

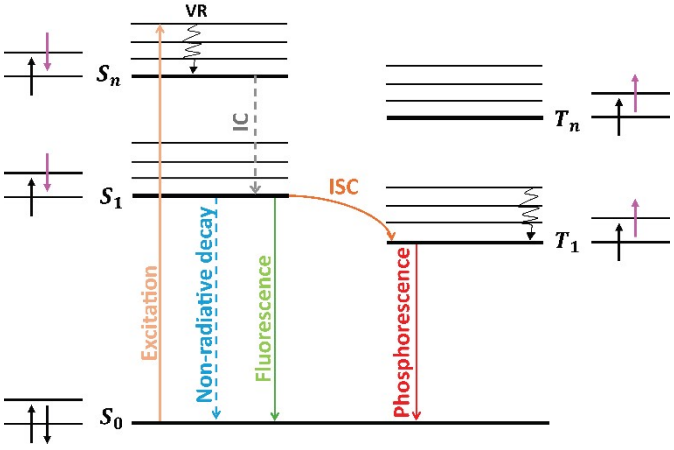

Fig. 2: Jablonski diagram indicating major photoluminescent transitions (VR: vibrational relaxation).

As per the El-Sayed rules, effective SOC and high rate of ISC (k_{ISC}) in pure organic systems requires preserved total angular momentum.[14] This means that a change in spin must be accompanied by a change in orbital type. For instance, a favourable transition may occur from an excited singlet state $^1(n,\pi^*)$ to a triplet state $^3(\pi,\pi^*)$. Here, one paired electron moves from a π orbital to a non-bonding (n) orbital and changes spin, resulting in two remaining unpaired π electrons of equal spin (Figure 3, top right corner). Similarly, a transition from $^1(\pi,\pi^*)$ to $^3(n,\pi^*)$, is favoured (Figure 3, top left corner). However, ISC from $^1(\pi,\pi^*)$ to $^3(\pi,\pi^*)$ or from $^1(n,\pi^*)$ to $^3(n,\pi^*)$ is unfavourable due to inefficient SOC and poor orbital overlap.[9] In addition to enhancing SOC, modifications that can reduce the singlet-triplet splitting energy (ΔE_{ST}) is another key factor controlling the rate of ISC, and this energy is dependent on the spatial overlap of the highest occupied molecular orbital (HOMO) and the lowest unoccupied molecular orbital (LUMO) wavefunctions.[15]

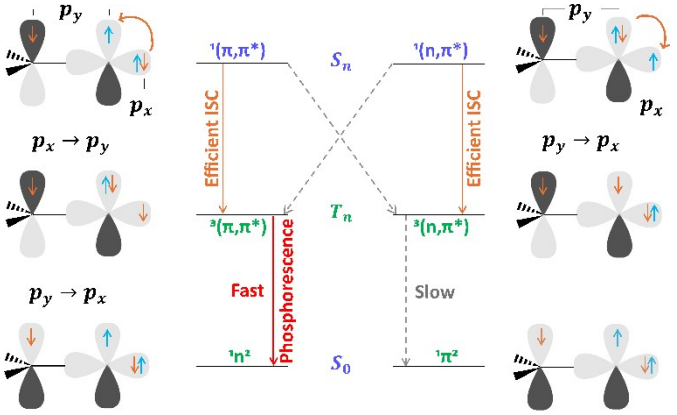

Fig. 3: Schematic of El-Sayed's rule exhibiting the enhanced phosphorescent decay when there is an orbital change.[9]

Hence, some common design strategies for purely organic RTP include the introduction of heavy atoms, and/or heteroatoms (such as oxygen, nitrogen, sulphur, and/or phosphorus) into the molecule to increase the number of n orbitals and enhance SOC.[5,16–19] By introducing lone-pair electrons, the S_1 state is given a dominant (n,π^*) characteristic and the closest T_n is given a dominant (π,π^*). This creates a large configuration difference in the proportion of n orbitals (α_n) and π orbitals (β_π) between S_1 and T_n, which leads to a larger SOC.[9] Aside from these strategies, the past few years have seen additional design principles such as crystallization, rigid matrix doping, polymerization, and supramolecular self-assembly in order to enhance the stability of the triplet excitons and suppress non-radiative decay.[1,12,13,16,20–22]

2. Functional RTP Materials

Significant research progress has been made on realizing purely organic RTP. However, more recent studies have delved beyond materials solely exhibiting RTP properties by introducing additional functionalities, herein defined as "functional RTP materials." In other words, these materials not only demonstrate effective phosphorescence under ambient conditions but are also purposefully designed towards specific applications. These properties include flexibility or dynamic/stimulus-responsiveness. Aside from these, functional materials also encompass a range of transductive qualities, such as scintillating behaviour or the ability to circularly polarize light.

In essence, functionalization broadens the scope of RTP materials by offering multi-scale processability and tunability.[23] For instance, Zhou et al. report the advantages of dynamic RTP systems, that are discussed in Section 2.2, over conventional static ones, such as their reversible sensitivity, quicker

response, and facile controllability.[24] Additionally, by introducing additional functionalities, RTP materials can be designed to meet specific industrial and/or application-driven demands. An example would be that of stretchable organic RTP materials. Traditionally, to suppress non-radiative transitions and molecular motions, crystal engineering and rigid matrices were employed, as highlighted previously. While this leads to enhanced phosphorescent emission, the brittle nature of these materials hinders their applicability to practical situations, such as wearable devices. Hence, flexible/stretchable RTP materials have been increasingly studied and have shown augmenting applications in the flexible electronics space and biomedical sensing.[25]

Aside from flexible systems, stimuli-responsive RTP materials may benefit the development of new phosphorescent sensors. As reported by Cai et al., sensors exhibiting strain or temperature-dependent RTP can function independently from complex electronic circuit systems.[26]

Functional purely organic RTP materials can further the scope of wearable and skin-like materials, moving towards higher biocompatibility and sustainability. Hence, these materials would be useful for the automation of medical sensing, even at room temperatures.[27] Overall, functionalization shifts RTP away from a theoretical framework and towards real-life applications, such as information storage and detection systems, among others, like X-ray imaging, that are discussed in further detail within Section 3 of this article.[28,29]

This article hence serves to examine recently reported literature on purely organic functional RTP materials that are flexible/stretchable, dynamic, scintillating and/or produce circularly polarized light. While previous works have touched upon different functionalities in isolation, herein we collate and discuss the major materials classes in a more comprehensive manner, and with respect to each other.[24,25,30] Moreover, we provide mechanistic insights and discuss potential limitations of some materials, highlighting certain considerations for future designs.

2.1 Flexible/Stretchable RTP Materials

Flexibility typically refers to the ability of a material to deform, and is demonstrated via bending, stretching, or softness.[31] While each of these terms have some variations in their implications, herein, flexibility and stretchability are considered similar aspects of a material and are thus analysed together. The extent of a material's flexibility is typically determined by the material's Young's modulus and its thickness, such that a significant reduction in the latter can even allow poorly deformable materials to exhibit some flexibility. The strain (ε) experienced by some material in the direction that it is bent/stretched is typically approximated by Equation 1, which exhibits the ratio of the stack thickness, including substrate (t_s) and film (t_f) thicknesses, to two times the radius of curvature (r). It should be noted that this is an approximation, and the actual strain of a material is far more complicated.[32]

$$\varepsilon = \frac{t_s + t_f}{2r} \quad (1)$$

As previously mentioned, the brittleness of rigid, inflexible RTP materials limits their real-world applications. However, rigidity is associated with enhanced RTP parameters, and thus achieving flexibility without losing RTP performance is intrinsically difficult. Earlier RTP materials specifically preferred rigid networks with strong molecular interactions and crystallization techniques to stabilize the triplet excitons and reduce vulnerabilities to quenching by air or moisture.[1,33] When placed under tensile stress, elastomeric chains may slowly straighten, leading to elastic deformation. After removing the external force, the polymer chains revert to their original state, causing them to possess relatively large free volumes that can hinder RTP. On the other hand, if this were to be combatted with increased inter/intra-molecular interactions, the material would be expected to be brittle. Hence, this class of RTP materials requires a balance between rigidity and flexibility.[33] These flexible RTP materials have been reported to have immense potential across various fields including flexible optoelectronics and data encryption, among others.[33–36]

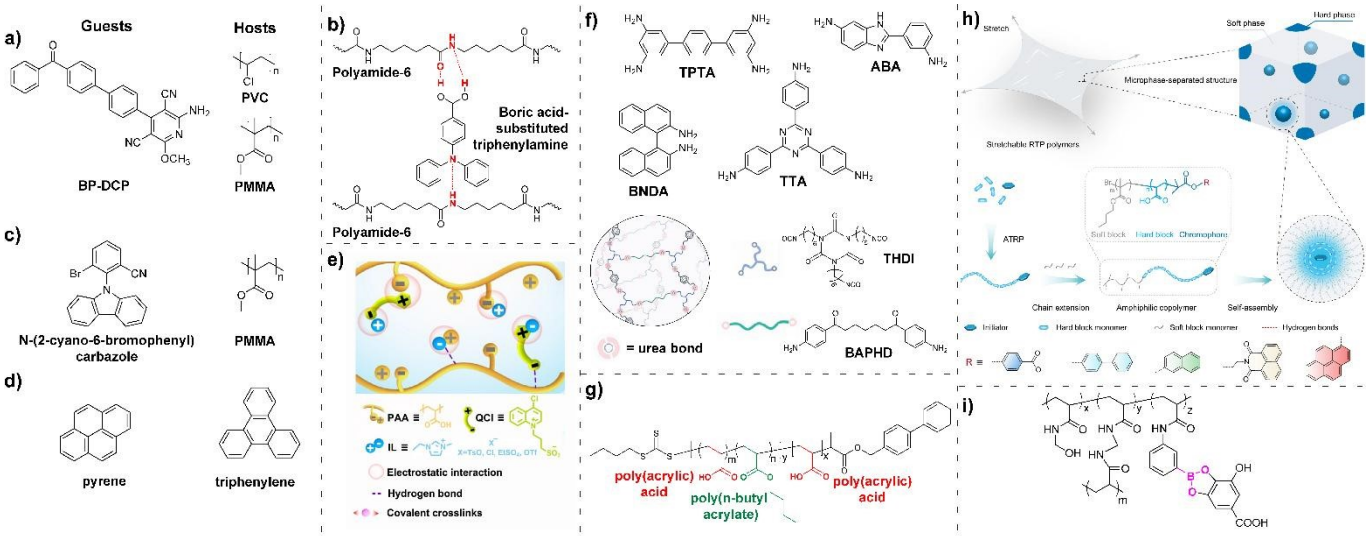

Fig. 4: Schematic of flexible organic RTP designs: a) BP-DCP guest molecule and PVC and PMMA hosts, b) hydrogen-bonding between a polyamide-6 matrix and a boric-acid substituted triphenylamine chromophore, (c) carbazole derivate guest molecule and PMMA host, (d) triphenylene host and pyrene guest used to create an organic crystal, (e) ionogel by Yang et al. (reprinted with permission[37]), (f) cross-linking schematic (bottom left) and multifunctional aromatic amines (reprinted with permission[38]), (g) a gradient copolymer, (h) multiphase engineering as a technique for stretchable RTP polymers (reproduced under a Creative Commons Attribution License (CC BY), copyright 2024[39]), and (i) a polymeric system with indicated B—O click chemistry (in pink).

View Article Online
DOI: 10.1039/D6TC00103

A common strategy to achieve flexible RTP materials is to dope phosphorescent chromophores within a stretchable polymer matrix which binds via intermolecular interactions, such as hydrogen bonding, ionic bonding, or other host-guest interactions.[25] In doing so, a locally microscopic rigid domain is created within the stretchable polymer matrix that stabilizes the phosphor's triplet states, ensuring efficient RTP while still allowing for elastic deformation by the dominant polymer matrix.[33] Host-guest systems can also involve molecules that are individually RTP inactive, but upon interaction lead to bright RTP; by ensuring that the rigid host and the phosphorescent guest are of compatible sizes, non-radiative transitions can be inhibited.[25,40,41]

Polyvinyl alcohol (PVA) is a widely employed polymer due to its many hydroxyl groups that can form controllable hydrogen bonding networks with the phosphorescent chromophores, thereby reducing molecular vibrations by creating a rigid microscopic domain. Moreover, PVA matrices are solution-processable and can be easily prepared as flexible films or fibres, facilitating their large-scale applications.[25] For instance, phenanthroline derivatives-doped PVA was observed to exhibit visible light-excited RTP with blue-green phosphorescence emission.[42] It is key to note that no intrinsic RTP behaviour was observed before integrating into the matrix, whereas, 5-amine-1,10-phenanthroline (one of the phenanthroline derivatives)-doped PVA showed high τ_p of 229.4 ms and Φ_p of 19.6%.[42]

Aside from PVA, other polymers have been reported for host-guest dopant systems, especially in the case of mechano-responsive materials (MRMs), that are discussed in further detail within dynamic RTP systems. For instance, electron donor dicyanopyridine (DCP) and electron acceptors benzophenone (BP) and 4-bromobenzophenone (Br-BP) were doped into PVA, polymethyl methacrylate (PMMA), and polyvinyl chloride (PVC) (Figure 4a).[35] Optimizing the host-guest doping ratios not only exhibited stretchability and strain-responsiveness, but also excitation wavelength-dependent RTP – in other words, the RTP properties were dependent on the wavelength used for excitation.[35] Results showed that the 1% BP-DCP@PMMA exhibited τ_p of 557.78 ms while the 1% BP-DCP@PVC film showed τ_p of 246.78 – 489.03 ms, pre- and post-stretching, and a tensile strength of 14.87 MPa. Similarly, Tao et al. examined MRMs with both mechanochromic and mechano-decay characteristics.[43] Via a melt-blending technique, commercial polymer polyamide-6 (PA6), which is rich in hydrogen bonding sites (Figure 4b), was doped with chromophores. The resulting polymer led to a dual emission of blue fluorescence and green RTP with a τ_p of 747 ms, with the RTP phenomenon being attributable to the hydrogen bonding interactions between the boric acid and imide groups within the chromophore and polymer, respectively. Furthermore, upon stretching/compressing the polymer, the intensity, colour, and lifetimes had changed, as macromolecular chains could move relative to each other.

Alternative polymeric doping strategies include additional thermoplasticizing.[44] For example, Yue et al. (Figure 4c) found that two carbazole derivative classes doped into a solution of PMMA led to poor RTP performance, but once thermoplasticized into plastic sheets, ultralong blue-yellow dual RTP was observed, with τ_p up to 1.38–1.77 s.[45]

Host-guest systems have also been reported in single flexible organic crystals among other supramolecular assemblies.[46] For instance, a racemic fluorenol-carbazole (PhOH-Cz) elastic π-conjugated molecular crystal exhibited an average elastic modulus of 8.42 GPa and hardness of 0.48 GPa – values that are comparable to conventional solid materials.[47] These single crystals also showed a relatively long τ_p of 94 ms with RTP spectra presenting a maximum at 555 nm. Similarly, Xia et al. integrated a triphenylene host, whose weak $\pi - \pi$ interactions allow for heightened flexibility, and pyrene as the guest (Figure 4d).[40] This host-guest system (9.2 GPa) retained the flexible nature of the host (Young's modulus of 8.9 GPa) and led to bright red RTP with a long emission lifetime of up to 405.9 ms in air.

Another novel class of flexible RTP materials is ionogels – polymer networks swelled with ionic liquids (ILs) – which utilize the high directivity and strength of ionic bonds to anchor phosphorescent chromophores onto the flexible matrix via electrostatic interactions, thus inhibiting non-radiative transitions.[48] Additionally, such materials tend to show dynamic behaviour as a result of the dynamic dissociation-recombination possibilities of ionic bonds.[25] Yang et al. combined a 3-(4-chloroquinolinium-1-yl)propane-1-sulfonate phosphor with an acrylic acid monomer, alongside a photo-initiator and an N, N'-methylenebisacrylamide cross-linker into 1-ethyl-3-methylimidazolium chloride ILs (among others) (Figure 4e) to form a precursor solution which was irradiated by UV for 5 minutes.[37] The obtained ionogel PAA-Cl(50) showed good performance, exhibiting a tensile strain of 497%, Young's modulus of 782 MPa, toughness of 111.2 MJ/m^3, and τ_p of 113.05 ms. Similarly, a salting-out-induced microphase separation mechanism was reported to lead to a "soft" IL phase that provides stretchability and ionic conductivity and a "hard" PVA polymeric matrix for enhanced RTP.[48] These ionogels showed close to 400% strain, around 20 MJ/m^3 toughness, ionic conductivity of 8.4 mS/cm and long afterglow lifetime up to 112.4 ms. In another recent study by Xu et al., they photopolymerized acrylic acid (AA) and N,N-diethylacrylamide (DEAM) in IL ([PMIM][PF6]) which was doped (≤ 0.1 wt%) by different organic phosphors. This resulted in a toughness of 77.11 MJ/m^3, as well as ultralong τ_p (> 4 s) for the majority of the ionogels, with the longest τ_p of 5.343 s being achieved for a 2% PP-5% AA-5% DEAM-doped with 0.1 wt% coronene.[49]

Similar to ionogels, another major class of flexible materials are hydrogels, which are hydrated 3-dimensional (3D) polymeric networks that are likened to body tissues, endowing them with high biocompatibility and stretchability.[50] One of the first reports of RTP hydrogels was that by Chen et al. who designed a supramolecular polymeric hydrogel that relied on the host-guest interactions between a β-cyclodextrin polymer host (poly-β-CD) and an α-bromonaphthalene polymer guest (poly-BrNp).[51]

Despite the great flexibility of RTP hydrogels, the presence of water poses an inherent challenge to the applicability of RTP hydrogels, as water can easily quench phosphorescence. Hence, different methods have been employed to stabilize triplet excitons and achieve effective RTP, despite this field still being at a nascent stage. A common method involves stabilizing, typically non-aromatic phosphors, by either ionic crosslinking or crystallization-induced clustering.[50,52–55] For instance, Deng et al. designed a PVA/poly(calcium maleate) (PMACa) non-aromatic phosphorescent hydrogel, that they dried under stretching ("DS" technique), which led to strong ionic and hydrogen bonds within the hydrogel structure. The system exhibited tensile strength of up to 15 MPa (water content 67.6%), modulus of 2.41 MPa, and a maximum τ_p of 13.4 ms.[52]

In general, while dopant strategies rely predominantly on hydrogen-bonding or ionic bonding interactions, polymerization is another strategy that relies on covalent bonds between the phosphorescent chromophores and stretchable polymer matrix. It enhances stability by further reducing vibrational/rotational losses due to phosphorescent molecule motion.[25] Cross-linked polymers have shown good RTP behaviour. For example, multifunctional aromatic amines were reacted with a hexamethylene diisocyanate trimer (THDI) crosslinking agent via a polycondensation reaction (Figure 4f), leading to preeminent tensile strengths up to 15 MPa and large elongation at break of around 120%.[38] These observations are explained by the carbonyl and nitrogen atoms enhancing the generation of triplet excitons, while the cross-linked network structure increased rigidity. Similarly, Cao et al. designed benzothiadiazole-based dialkene phosphor molecules that were also initiators and crosslinkers to produce a range of flexible phosphorescent gels (organogels, ionogels, aerogels, and hydrogels).[56]

Copolymerization has been increasingly reported for applications in tuneable RTP, as matrix rigidity correlates with polymerization degree that can be easily tuned by exerting control over the polymerization reaction conditions.[2,39] A representative study by Ma et al. highlighted the benefits of copolymeric structures for RTP, where copolymerization of acrylamide with different phosphors led to a cross-linked hydrogen-bonding network that immobilized the phosphors and shielded them from quenchers.[57] More recently, a reversible deactivation radical polymerization technique was employed to synthesize a gradient copolymer (GCP) (Figure 4g). This polymer combined a poly(n-butyl acrylate) [P(n-BA)] "soft segment" with a poly(acrylic acid) (PAA) "hard segment" using biphenyl reacted with 2-butylsulfanyl-thiocarbonylsulfanyl-propionic acid (a chromophore-labelled chain transfer agent) as the chromophore. This system exhibited tuneable stretchability, effective RTP, and was healable post-stretching.[58] Mechanically, the polymer offered tuneable elongation at break from 5.0% to 221.7% and a Young's modulus from 0.5 to 225.0 MPa.

Likewise, a stretchable, ultralong copolymer of 4,4'-methylenedicyclohexyl diisocyanate, poly(tetrahydrofuran), and adipic dihydrazide covalently bonded to a polyurethane backbone led to a maximum strain of 1400% (for Sample PPU-0.2) and τ_p of 1888 ms (for Sample PPU-0.35).[59] This backbone served to provide both the "soft segments," which comprise the polyether or polyester polyols that contribute to the tensile properties, and the "hard segments," which consist of the polar urethane or urea groups that enhance structural rigidity.

A key study by Gan et al. reported that, as a result of microphase separation, their multiphase-engineered copolymer structures (Figure 4h) demonstrated a stretchability of 712% while maintaining a τ_p of up to 981.11 ms.[39] This method of integrating multiple functions into the block copolymer facilitated the achievement of a low glass transition temperature (T_g), which is required for stretchable systems and is not easily achievable.

While this covalent binding approach is well-documented in literature, some studies point out its low feasibility in terms of scalability due to the reliance on complex synthetic procedures.[47] Hence, other techniques have been proposed, such as click chemistry, which combats the binding engineering aspects and time-consuming nature of covalently binding the phosphors to the polymer.[60] B-O click reactions (Figure 4i), for instance, extend the p-conjugation system via the vacant p_z^0 orbital of boron, reducing the energy gap between the lowest excited singlet and triplet states.[61,62] Yang et al. reported a polymer that employed this B-O click chemistry which achieved a maximum τ_p of 629.29 ms and ϕ_p of 1.9 %.[61]

Table 1 below summarizes the various methods discussed within this section to provide an overview of the τ_p, tensile strains, moduli, and/or strengths. Unfortunately, many studies do not report all these parameters despite designing flexible/stretchable materials, implying the need for a standardized reporting system.

Nonetheless, overall, it appears that longer lifetimes are achieved when phosphors are covalently bound (typically by copolymerization) to the rigid matrix. These systems also exhibit excellent strains, allowing for effective flexibility. It is also confirmed that systems that offer greater tensile strains at break tend to offer lower moduli, and vice versa.

View Article Online
DOI: 10.1039/D6TC00010J

Table 1: Comparative summary of flexible RTP systems

Strategy	Composition	τ_p	Tensile Strain	Modulus	Strength	Ref.
Host-guest doped polymer	5-amine-1,10-phenanthroline-doped PVA	229.4 ms	–	–	–	42
	BP-DCP-doped PVC	246.78 – 489.03 ms	137.38% (elongation at break)	–	14.87 MPa	35
	Boric-acid substituted triphenylamine-doped PA6	747 ms	~ 220% (at break)	–	–	43
	Pseudopolyrotaxane-doped waterborne polyurethane	762.34 ms	812% (fracture strain)	8.6 MPa	–	63
Thermoplasticized polymer	Carbazole derivative-doped PMMA	1380 – 1770 ms	–	–	–	45
Single flexible organic crystals	PhOH-Cz	94 ms	–	8.42 GPa	–	47
	Pyrene-doped triphenylene	409.7 ms	–	9.2 GPa	–	40
Ionogel	PAA-Cl(50)	113.05 ms	497%	782 MPa	53 MPa (yield strength)	37
	PVA/polyacrylamide-salted out by CO_3^{2-}	112.4 ms	425.3%	–	9.14 MPa	48
Hydrogel	PVA/PMACa-DS	13.4 ms	–	2.41 MPa	15 MPa	52
Chemically-crosslinked polymers	BNDA@PU	972.3 ms	120% (elongation at break)	–	15 MPa	38
Copolymerization	Organic quaternary phosphonium derivatives, acrylamide, 2,2,2-trifluoroethyl acrylate	659.0 ms	500%	–	–	34
	PAA, P(n-BA), biphenyl	1180 ms (GCP-3)	221.7% (GCP-4; elongation at break)	225.0 MPa (GCP-1)	6.0 MPa (GCP-1)	58
	4,4′-methylenedicyclohexyl diisocyanate, poly(tetrahydrofuran), and adipic dihydrazide bonded to polyurethane	1888 ms	200%	95.4 MPa	26.1 MPa (stress)	59
	PNPy	981.11 ms (PNPy-1)	712% (PNPy-3; at break)	97.8 MPa (PNPy-1)	10.5 MPa (PNPy-1; at break)	39
	Acrylamide and N-[4-(9H-carbazol-9-yl) phenyl]-2-propenamide	503 ms	452%	–	5.1 MPa	64
Click reactions	Poly(N-methylolacrylamide-*co*-3-acrylamidephenylboronic acid)-gallic acid	629.29 ms	–	–	–	61

Note: (–) indicates that this parameter has not been explicitly reported in the cited literature.

2.2 Dynamic RTP Systems

The traditional static RTP materials typically involve those that have non-tuneable photophysical properties, while the more novel dynamic materials showcase stimuli-responsive characteristics under specific stimuli, such that they provide more benefits over static materials.[24] According to Zhou et al., static materials exhibit only macroscopic changes upon exertion of an external stimulus, and no changes in their photophysical properties.[24] Meanwhile, dynamic materials show both macroscopic and microscopic structural changes and hence exhibit modifications to their optical and physical properties, as is reported for various carbon dots-based RTP materials.[65,66] Many material classes fall under the umbrella of dynamic stimuli-responsive materials, including responsiveness to heat, light, force, strain, and pH.[67–70]

Mechanochromic materials are a major class of dynamic RTP materials whose emissive properties can be manipulated by mechanical force. Consequently, these materials have shown promising applications within the physical detection space.[71] Huang et al. report that such materials emit different colours based on molecular isomerization, molecular packing mode modifications, or molecular conformational changes. These factors imply that, despite RTP being achievable in an amorphous matrix, a phase transition via mechanical grinding leads to quenching of the triplet excitons, resulting in RTP tuneability.[72]

View Article Online
DOI: 10.1039/D6TC00010J

HIGHLIGHT

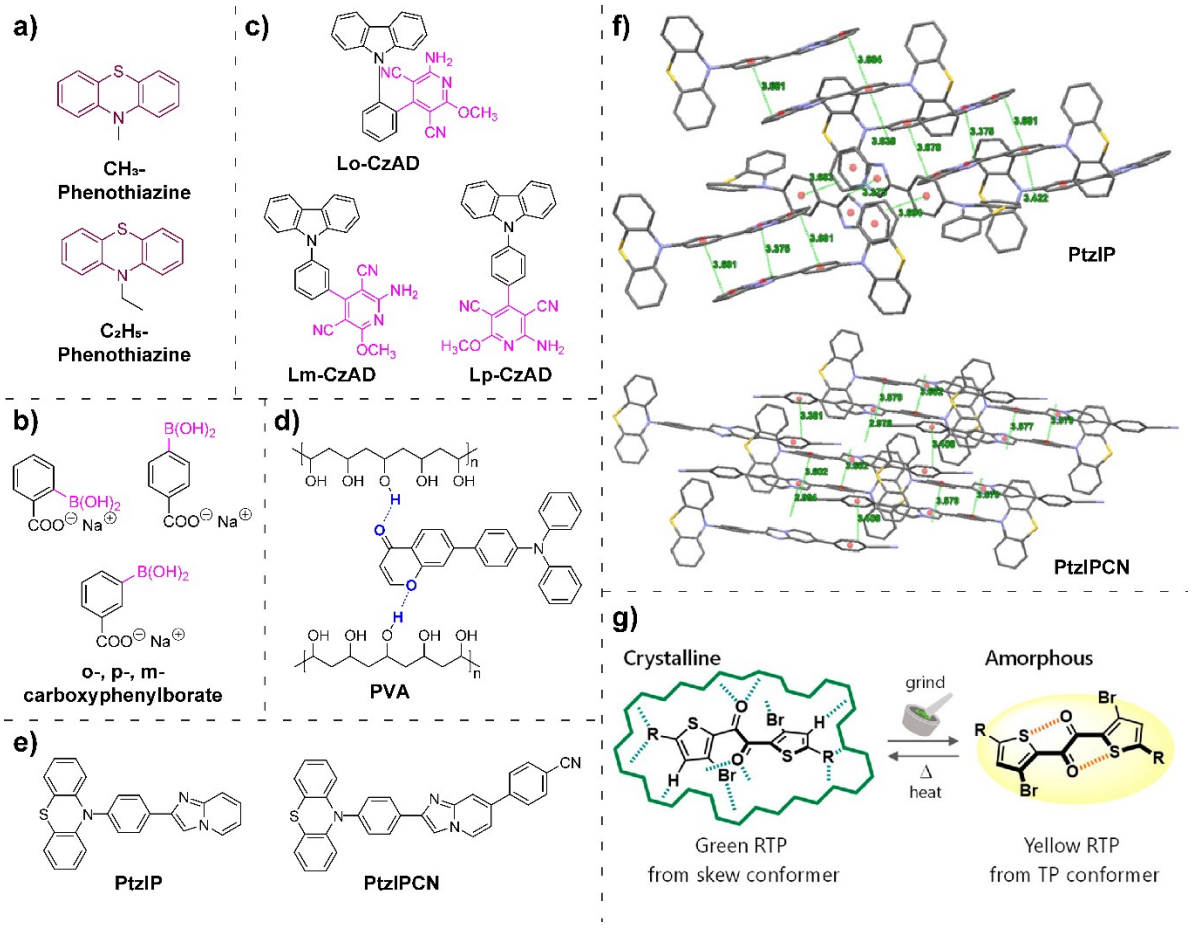

Fig. 5: Schematic of mechanochromic organic RTP systems: a) phenothiazine derivatives, b) isomerism-dependent mechanochromism, c) clustering-induced mechanochromic carbazoles, d) hydrogen bonding between a 4H-chromenone (center) and a PVA matrix, e) structures of PtzIP and PtzIPCN, f) intermolecular $\pi - \pi$ stacking for PtzIP and PtzIPCN (reproduced with permission[73]), g) RTP-to-RTP mechanochromism (reproduced under a Creative Commons Attribution License (CC BY), copyright 2022[74]).

Some early examples of mechanochromic RTP include phenothiazine-based systems (Figure 5a) leading to high-contrast mechanochromism and a change in the photoluminescence colour, and benzophenone-aromatic amine conjugates that possess a twisted donor-acceptor framework to facilitate mechanochromic RTP.[75,76] A recent example of mechanochromic RTP is that by Nie et al. who designed a new class of organic ionic crystals using a structural isomerization strategy (Figure 5b), relying on variations in RTP due to transformations of the molecular arrangement.[77] Their materials exhibited ultra-long RTP (longest τ_p of 732.8 ms observed for the meta-isomer crystal) and mechanochromic emission after grinding. The authors observed that by grinding the ortho-isomer crystal, green and orange phosphorescence was observed before and after removing the excitation source, respectively. Additionally, the emission maxima of the prompt and delayed spectra were redshifted, with τ_p increasing from 6.1 ms to 125.4 ms upon grinding, and ϕ_p increasing from less than 0.01% to 1.5%.

This clustering-induced or isomerism-dependent phosphorescent systems was also observed by Guo et al., who combined three carbazoles – commonly used as planar electron donors with high triplet energy levels – with 3,5-dicyanopyridine (DCP) (electron donor) to form three crystal structures, namely Lo-CzAD, Lm-CzAD, and Lp-CzAD (Figure 5c).[78,79] Their results showed that mechanochromism varied based on the isomerism of the starting carbazole unit with crystal Lo-CzAD showcasing the best RTP performance as demonstrated by the obtained τ_p of 187.16 ms and afterglow of 1 s, while only Lp-CzAD showed reversible (by heating) mechanochromic activity before/after grinding. This is attributed to a phase transition between the crystalline and amorphous states, while the other two crystals showed mechanochromic inertness due to their high crystallinity.

Mechanochromic RTP behaviour, as is with flexible RTP materials, can be induced through host-guest doping strategies, for instance, via integrating 4H-chromenones in a PVA matrix (Figure 5d).[80] These triphenylamine derivatives improved the degree of molecular conformational distortion which can tightly stack after grinding, leading to enhanced mechanochromism; a deviation from conventional crystalline-amorphous transitions leading to mechanochromic behaviour. Their carbazole-based guests did not exhibit mechanochromism despite transitioning from crystalline to amorphous states post-grinding due to the irregular stacking when ground as opposed to the organized stacking observed for the triphenylamine derivatives.

A 2021 study by Li et al. examined 9,10-dihydro-9,9-dimethylacridine (DMAC) that could form two different conformations as an electron donor, with dibenzothiophene 5,5-dioxide (DBTDO) as an electron acceptor.[81] They also compared DMAC with 2-(cyclohexa-2,4-dien-1-yl(phenyl)amino) and 2-(4a,9a-dihydro-9H-carbazol-9-yl). Two polymorphs of DBTDO-DMAC were obtained, with the crystal with planar conformation showcasing mechanochromism.

Another study examined two phenothiazine-based luminogens PtzIP and PtzIPCN (Figure 5e) in which the former showed mechanochromic response and tuneable RTP at specific wavelengths while the latter did not in its crystalline state – this difference is attributed to PtzIPCN being more crystallisable than PtzIP and the reduced intermolecular $\pi - \pi$ stacking in the latter (Figure 5f).[73] When combined with a PMMA host or a 4-fluorobenzophenone (F-BP) host, the doped systems showed concentration-dependent fluorescence and phosphorescence emissions with τ_p up to 185.31 ms for PtzIPCN@PMMA and 216.63 ms for PtzIPCN-doped F-BP at a doping ratio of 1:1000 PtzIPCN:F-BP.

While mechanochromism-activated or deactivated RTP is commonly reported, RTP-to-RTP by mechanochromism is not as commonly discussed; this type of mechanochromism shows different RTP colours pre- and post-grinding. For instance, Takewaki et al. synthesized a thienyl diketone called ClTn, similar to their previous work[82] using bromines (Figure 5g) which exhibited green RTP in crystalline form and yellow RTP when amorphous.[74] Using a halogen-exchange strategy, they observed RTP-to-RTP mechanochromism, as opposed to the typical mechanical quenching or enhancement observed for conventional organic phosphors. In other words, mechanical stimuli led to amorphization which manifested in an RTP colour change.

Photo-responsive materials is another well-documented class of materials.[83] An early study demonstrated that prolonged irradiation of carbazole-based organic phosphors PCzT, BCzT, and FCzT led to photoactivated RTP with τ_p ranging from 1.8 to 1330 ms.[84] These phosphors could also be deactivated via UV irradiation for 3 hours or by thermal treatment.

View Article Online
DOI: 10.1039/D6TC00010J

HIGHLIGHT

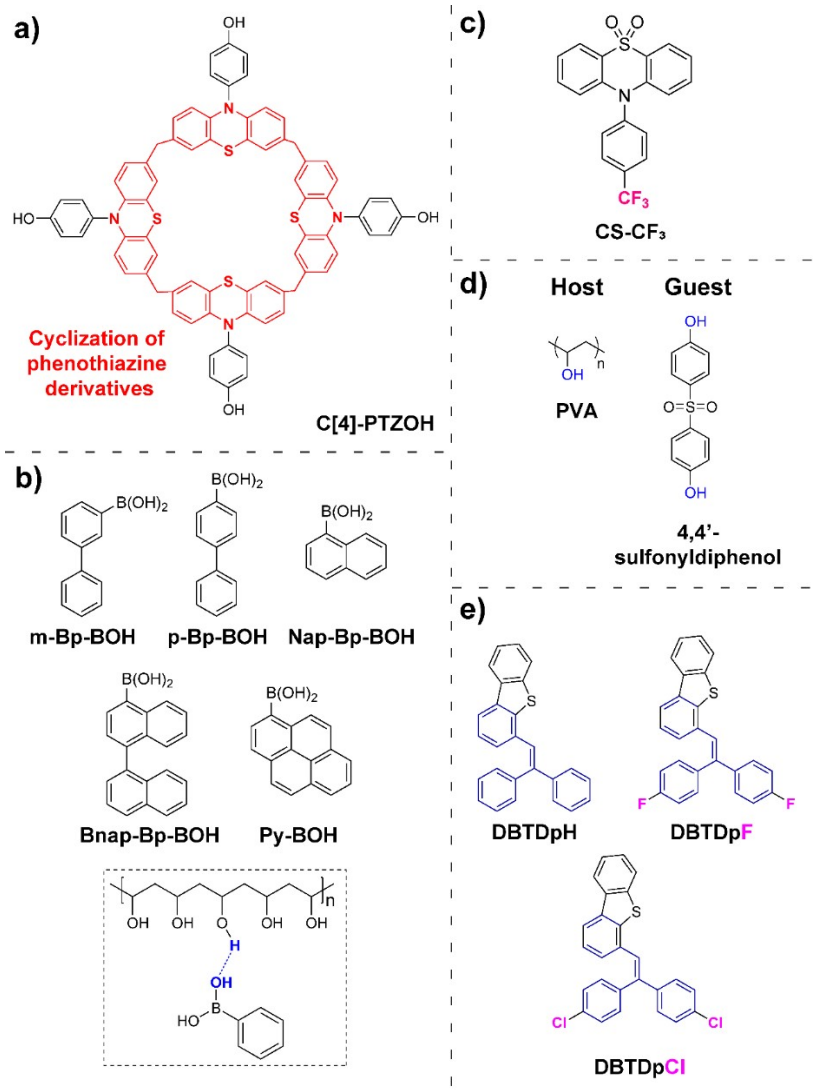

Fig. 6: Schematic of organic RTP systems exhibiting light-responsiveness: (a) cyclization of phenothiazine derivatives, (b) arylboronic acids (top) and example of hydrogen bonding (bottom), (c) -CF_3 group-substituted 10-phenyl-10H-phenothiazine-5,5-dioxide-based derivative, (d) an SDP guest and PVA host, and (e) triphenylethylene derivatives.

Recently, reports of cyclization-enhanced mechanisms for photoactivated RTP have been observed. For instance, Sun et al. integrated cyclized phenothiazine derivatives into an amorphous PVA matrix (Figure 6a).[85] This integration led to improved dynamic RTP in comparison to the pristine monomers. Results showed that τ_p and ϕ_p of the cyclized derivative increased from 11.8 to 23.1 ms and from 8.62% to 29.53%, respectively, with respect to the non-cyclized structure. This drastic augmentation is attributed to the greater rigidification by cyclization, suppressing non-radiative transitions and increasing ISC, as well as the extensive hydrogen-bonding network between the phenothiazine groups and PVA. Additionally, the structure isolates the system from oxygen and moisture, proving effective against quenchers under irradiation.

Varying the irradiation wavelengths can also affect the RTP behaviour of certain pure organic systems, demonstrating colour-tunability.[86] As an example, hydrogen bonding between arylboronic acids with varying conjugated systems and a PVA matrix led to excellent RTP performance (Figure 6b).[87] More importantly, the RTP was excitation-dependent, in which the afterglow colour changed from blue to green to red as excitation wavelength increased. Additionally, the RTP

behaviour was observed to be water and heat-sensitive due to the system's rigidity being vulnerable to breakage by water.

Light-responsive RTP materials also include a class of structures that exhibit variations in RTP behaviour based on the duration of the irradiation, with increased durations of UV irradiation tending to increase RTP parameters, up to a certain threshold.[88–90] Such materials were first reported by Yang et al. in 2018 who synthesized seven 10-phenyl-10H-phenothiazine-5,5-dioxide-based derivatives with strong $\pi - \pi$ interactions in the solid state which promoted persistent RTP.[91] Specifically, the -CF_3 substituent led to high electron-withdrawing character that could further facilitate $\pi - \pi$ interactions, making the crystal exhibit unique photo-induced phosphorescence due to variations in molecular packing (Figure 6c). Intrinsically, the powder showed no visible RTP, however, once irradiated by UV for 5 minutes, it showed persistent RTP with long τ_p of 299 ms, only returning to the initial state after many hours.

In the same year, Su et al. designed a hexa-(4-carboxyl-phenoxy)-cyclotriphosphazene-doped PVA matrix.[92] A key takeaway from their analysis was that, upon increasing the duration of UV irradiation from 0 to 65 minutes at 298 K, τ_p and ϕ_p increased from 0.28 to 0.71 s and from 2.85 to 11.23%, respectively. When the duration went beyond 65 minutes, however, they observed decreases to τ_p among other properties. Temperature was also considered, albeit τ_p not significantly varying when temperature was changed to 77 K (0.88 s). Similarly, a study in 2021 observed that 4,4′-sulfonyldiphenol (SDP)-doped PVA films (Figure 6d) exhibited a 14.3-fold enhancement in τ_p from 58.03 to 828.81 ms after 45 minutes of UV irradiation, but weaker phosphorescence when irradiated beyond this duration.[93] In a PMMA matrix, no obvious phosphorescence nor irradiation-enhanced phosphorescence emissions were seen before and after 45 minutes of irradiation. Such behaviour is explained by two key reasons: Firstly, UV irradiation causes oxidation of the PVA hydroxyl groups, resulting in oxygen radicals. These radicals can form complex cross-linked ether structures that can suppress non-radiative transitions thereby enhancing RTP. Secondly, prolonged irradiation – albeit promoting cross-linkage – ultimately reduces the hydrogen bonding interactions between the dopant and the PVA matrix. This increases non-radiative transitions and reduces RTP performance.

While UV-activated phosphorescence has long been of interest, more recent studies have examined the use of visible light for RTP. Visible-light responsive RTP materials, which showcase more red-shifted absorption and potentially enhanced inhibition of non-radiative dissipation, combat the photoaging effects associated with traditional UV light-excited materials, as well as offer lower phototoxicity and deeper penetrability, making practical applications more feasible.[94]

Xiao et al. recently synthesized three triphenylethylene derivatives based on a host-guest inclusion design strategy (Figure 6e).[95] This system exhibited both visible light-triggered photochromism and RTP dual-functional properties that were attributed to the extended π-conjugated structure of triphenylethylene derivatives in a ring-closed form, leading to red-shifting of the absorption and excitation spectra. Additionally, the presence of halogens increased intermolecular interactions that stabilize triplet excitons, allowing for the visible light-activated photochromism and RTP behaviour to be observed.

Apart from mechanical grinding and light, many RTP materials have also shown responsiveness to heat/temperature variations, with changes to RTP depending on the balance between kinetics and thermodynamics, effectively increasing or decreasing RTP properties.[96–99] For example, water and heat-sensitive RTP materials made from covalently linking arylboronic acid phosphorescent chromophores to a PVA matrix exhibited ultralong τ_p of 2.43 s at 80 °C and ϕ_p of 7.51%.[100] The sensitivity arose from the hydrogen bonding between adjacent PVA polymers that could, in effect, modify the rigidity of the overall system. A seminal study in 2017 showed that two RTP materials (SHB_2t and SDB_2t) synthesized using Suzuki coupling reactions, led to efficient RTP via a strong intermolecular H-bonding, related to the angular arrangement ("butterfly structure"), and the SOC of the sulfonyl oxygen atoms. These materials also exhibited reversible mechanochromism and thermochromism between white, blue, and deep-blue emission.[97]

A recent study capitalized on the Förster resonance energy transfer (FRET) to design a stimulus-responsive RTP system as a result of the FRET system's specificity and sensitivity – these materials exhibited "turn-on" RTP when exerted upon by force or heat.[101] A N,N-dimethylpyridin-4-amine (DMAP) host – which has an abundance of nitrogen atoms to favour hydrogen bonding – and a di-(naphthalen-2-yl)-amine (Cdp) guest were employed, and this system was observed to exhibit a "turn-on" RTP effect post-grinding, suggesting mechanochromic behaviour. In addition, the system was heated, accelerating the acceptor and donor molecules closer to each other for enhanced FRET, manifesting in variations in RTP. At 25°C, there was no apparent RTP emission, but increasing temperature promoted a FRET process between DMAP and Cdp, leading to a longer afterglow (more than 4 seconds) of the Cdp molecule after heating at 110°C for around 10 min. Moreover, ϕ_p and τ_p were observed to be 3.16% and 756 ms, respectively, clearly demonstrating heat-responsiveness.

2.3 Scintillating RTP Systems

Scintillation refers to the conversion of high-energy radiation (X-rays, in this case) into low-energy visible radio-luminescence. X-rays are associated with high spatial resolution, low phototoxicity, and deep tissue penetration.[102] While flexible and dynamic RTP materials are increasingly reported in literature, X-ray scintillating RTP materials are a far more novel class of transductive functional materials. The mechanism of X-ray scintillation by organic systems involves X-ray photons interacting typically with heavy atoms within the organic molecules via a photoelectric effect and Compton scattering, leading to electrons and holes being generated. The electrons, which are high in energy, can subsequently collide with other atoms via an electron-electron scattering process/Auger process, leading to the generation of multiple

View Article Online
DOI: 10.1039/D5TC00101

secondary electrons. This is followed by electron-hole recombination to form excitons, somewhat like organic light-emitting diodes (OLEDs), that can participate in RTP (Figure 7a, right)[103]. RTP scintillators surpass conventional fluorescent scintillators which effectively utilize only around 25% of the singlet excitons under X-ray excitation, while RTP can theoretically utilize 100% (both triplet and singlet excitons)[104] – this concept is further explained within the Applications section.

In the case of X-ray scintillators based on RTP materials, many organic RTP phosphors have been reported to demonstrate effective X-ray scintillation.[103] These materials have a wide range of potential applications, from radiation detection to security inspection and even X-ray astronomy.[105]

The earliest study was reported in 2020 by Tang et al., who synthesized X-ray-excitable organic ultralong RTP materials for afterglow scintillators (Figure 7b).[102] The materials relied on intramolecular charge transfer enhancing $n-\pi^*$ transitions from the carbonyl moieties to the phenyl rings of the carbazole groups – results showed that the molecules showed τ_p up to 790 ms, ϕ_p of around 8%, and "excellent scintillation stability".

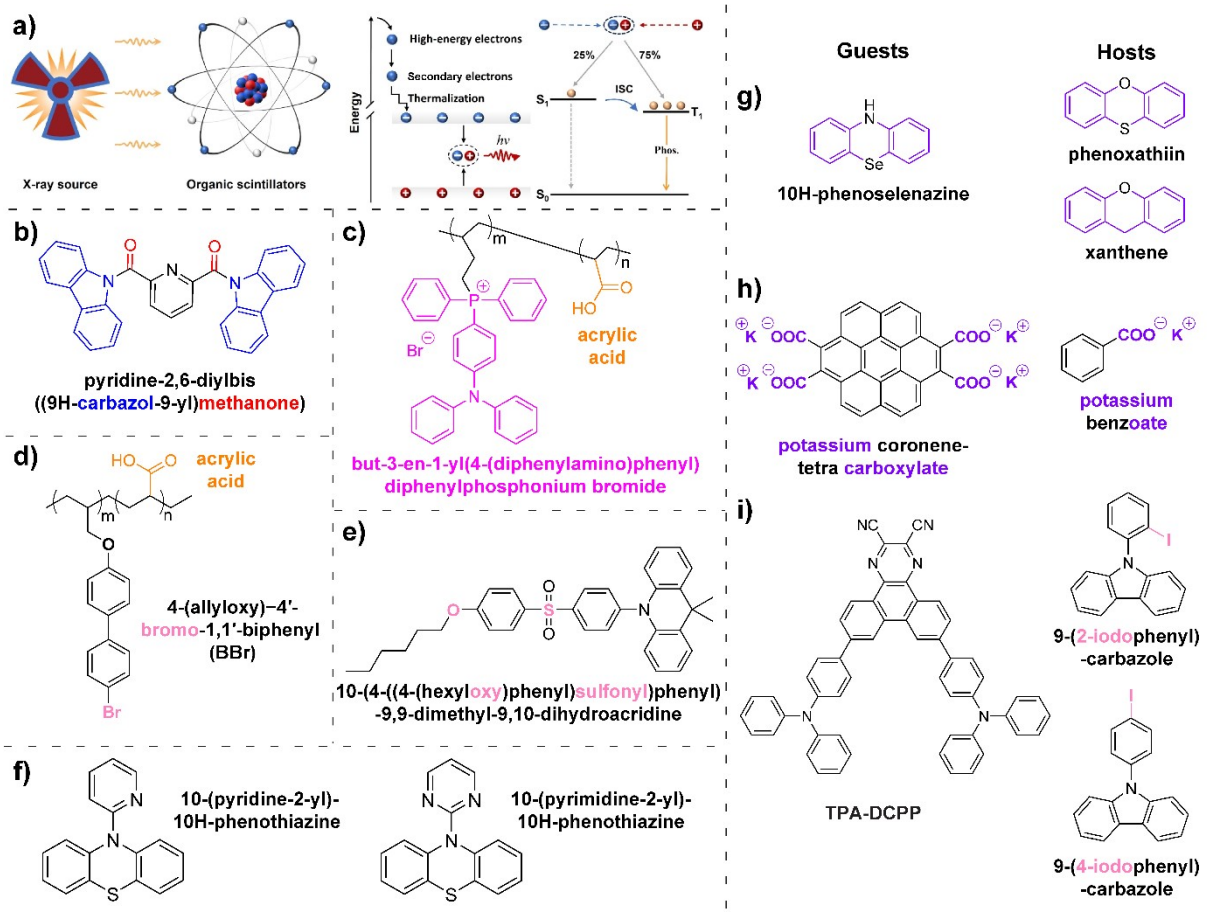

Fig. 7: (a) Schematic of the mechanism of X-ray scintillation as manifested in phosphorescent systems (right) (reproduced with permission[103]); Schematic of organic RTP systems exhibiting X-ray scintillation: (b) carbazole and carbonyl moieties involved in intra-molecular charge transfer, (c) copolymer of an organic quaternary phosphonium derivative in a rigid matrix, (d) copolymer with acrylic acid and a bromine-containing molecule, (e) molecule with sulphur and alkoxy oxygen groups, (f) polymorphism-dependent structures, (g) chemically similar hosts and guests, (h) ionic host and guest, and (i) isomerism-dependent hosts and guest.

A common design strategy for X-ray scintillating RTP materials is to synthesize RTP polymers, which offer a range of benefits over small molecules, such as large-area processability, flexibility, and reproducibility.[106] For example, a copolymer of quaternary phosphonium salt and acrylic acid possesses RTP because due to strong intermolecular electronic coupling, and showed multiple emission colours (Figure 7c).[106] One of the polymers showcased high photostability under high X-ray irradiation dosage of 27.35 Gy with a detection limit of 149 nGy/s – lower than that of traditional anthracene-based scintillators. Copolymerization of negatively charged polyacrylic acid and positively charged triphenylphosphine salts also showed good photostability under a high X-ray irradiation dosage and a low detection limit of 149 nGy/s.[107] Similarly, Gan et al. designed bromine-substituted chromophores and acrylic acid-based polymers (combined via free-radical copolymerization) that showed efficient X-ray responsiveness and ϕ_p up to 51.4% (Figure 7d).[108] This performance was attributed to the phosphorescent emission of the isolated 4-(allyloxy)−4'-bromo-1,1'-biphenyl (BBr) chromophores within the copolymeric structure.

Implementation of the heavy-atom effect has shown promising X-ray scintillating RTP enhancement.[109] Taking advantage of the high atomic number (Z-value) of the sulphur

View Article Online
DOI: 10.1039/D5TC00810J

atom that could also preferentially absorb X-rays, a range of sulfone-based organic molecules were designed using an alkoxy chain engineering technique on the prototype molecule mono-Bis[4-(9,9-dimethyl-9,10-dihydroacridine)phenyl]sulfone (mono-DMACDPS).[104] In addition to the sulphur group, the oxygen atoms in the alkoxy chain (Figure 7e) facilitated ISC and enhanced $n-\pi^*$ transitions, with varying chain lengths inducing variations in molecular packing. Alongside demonstrating effective molecular-packing-dependent RTP and one of their structures exhibiting high X-ray imaging resolutions of 15.0 and 10.6 line pairs/mm, these structures integrated both thermally activated delayed fluorescence (TADF) and RTP aspects to showcase enhanced scintillating behaviour.

In addition to these strategies, recent research has investigated other techniques such as polymorphism-dependence, which was observed in two phenothiazine derivatives, 10-(pyridine-2-yl)–10H-phenothiazine and 10-(pyrimidine-2-yl)–10H-phenothiazine (Figure 7f), in which the solvent system and molecular stacking had an impact on the scintillator triplet excitons' non-radiative transitions.[110] These phosphorescent scintillators, which also incorporated the heavy-atom effect, showed low detection limits of 278 nGy/s.

Host-guest dopant strategies have also been recently explored for enhanced scintillating RTP behaviour. In the work by Zhou et al., 10H-phenoselenazine (PZ) was selected as the guest while thianthrene (TA), phenoxathiin (PT), xanthene (XT), and carbazole (Cz) were selected as hosts, as they are structurally similar to PZ (Figure 7g).[111] These structures include heteroatom-bridged heterocycles which can enhance ISC and populate triplet excitons. The longest τ_p of around 1.8 ms was observed for PZ/XT and the highest ϕ_p of 99.4% was observed for PZ/PT. Moreover, integration of the host led to significantly higher radioluminescence under X-ray irradiation for all guest molecules, with a high X-ray attenuation efficiency of 58% achieved for 0.3 cm thick PZ/PT, also due to the presence of heavy atoms. PZ/PT was also observed to exhibit a lowest detectable dose rate of 77 nGy/s, further confirming the benefit of confining chromophores into rigid hosts.

Organic ionic host-guest phosphorescence systems have also shown to be effective in exhibiting X-ray scintillating RTP as ionic bonds can offer enhanced intra- and intermolecular interactions that can further stabilize excitons. For example, Wang et al. reported a ϕ_p of 38.7% and ultrahigh-temperature-resistant dual emissions, with low X-ray detection limits of 71.5 nGy/s (Figure 7h).[112] However, it is important to optimize the selection of hosts, when designing host-guest systems for scintillating RTP behaviour.[113] For example, two similar hosts, 9-(2-Iodophenyl)-9H-carbazole (oIPhCz) and 9-(4-Iodophenyl)-9H-carbazole (pIPhCz) (Figure 7i), were compared, and the mere modification of the position of the iodine atom translated into RTP being detected in oIPhCz but not in pIPhCz. Under X-ray excitation, oIPhCz showed detectable phosphorescence while pIPhCz showed no phosphorescence.[113] These variations were ascribed to higher SOC values for oIPhCz than pIPhCz, leading to better ISC, as per time-dependent DFT calculations. Isomeric positions plays a key role in the heavy-atom effect which variations being attributed to the effective crystal packing of these isomers, affecting conductivity and consequently electron-hole recombination.[114]

While these RTP scintillators have shown vast applicability across different X-ray imaging applications, as it outlined in Section 3, the inherently long lifetimes of RTP scintillators may prove detrimental to high-speed X-ray imaging in fields like medical diagnostic radiology.[115,116] For such applications, short photoluminescent decay lifetimes and bright emissions are essential to avoid issues like image ghosting.[115] One potential workaround for RTP systems to provide high yields with shorter lifetimes is the integration of heavy atoms, and specifically, halogen atoms. Heavy atoms like iodine tend to effectively reduce τ_p while maintaining high ϕ_p, potentially making these structures ideal candidates for high-speed X-ray applications.[117,118] However, designs would need to account for the low chemical stability when these systems are exposed to thermal and/or electrical treatments.[119]

Alternatively, opting for "hot exciton" scintillators, as reported by various researchers, can offer ultrafast decay and high yields, realizing practical high-speed X-ray imaging.[103] Zhang et al. demonstrated that hybridized local and charge-transfer excited states can enable high-level triplet to singlet reverse ISC transitions, reducing lifetimes and enabling the theoretical use of 100% of the generated excitons (readers are directed to Section 3 for a more in-depth discussion of this principle of using all excitons).[116]

2.4 Circularly Polarized RTP Systems

Circularly polarized (CP) materials have been increasingly studied in literature as a response to the disadvantages of obtaining CP light via the conventional linear polarizer and quarter-wave plate, such as the intrinsic complexity and associated energy losses.[120] CP photoluminescence is achieved by irradiating chiral luminescent molecules with non-polarized light, preferentially tuning the materials to achieve right or left-handed polarization. This concept has led to the development of CP RTP due to their longer exciton lifetimes and distinct CP photoluminescence characteristics, with vast applications such as organic chiroptical optoelectronics or displays. [30,121]

The efficacy of CP RTP is measured by the luminescent dissymmetry factor g_{lum} (Equation 2) where I_L and I_R refer to the luminescence intensity of left and right-handed CP phosphorescence, respectively:[31]

$$g_{lum} = \frac{2(I_L - I_R)}{I_L + I_R} \quad (2)$$

There are many ways to design CP RTP materials, including the incorporation of chiral chromophores, self-assembly, and host-guest doping, among others.[30,122]

View Article Online
DOI: 10.1039/D6TC00010J

HIGHLIGHT

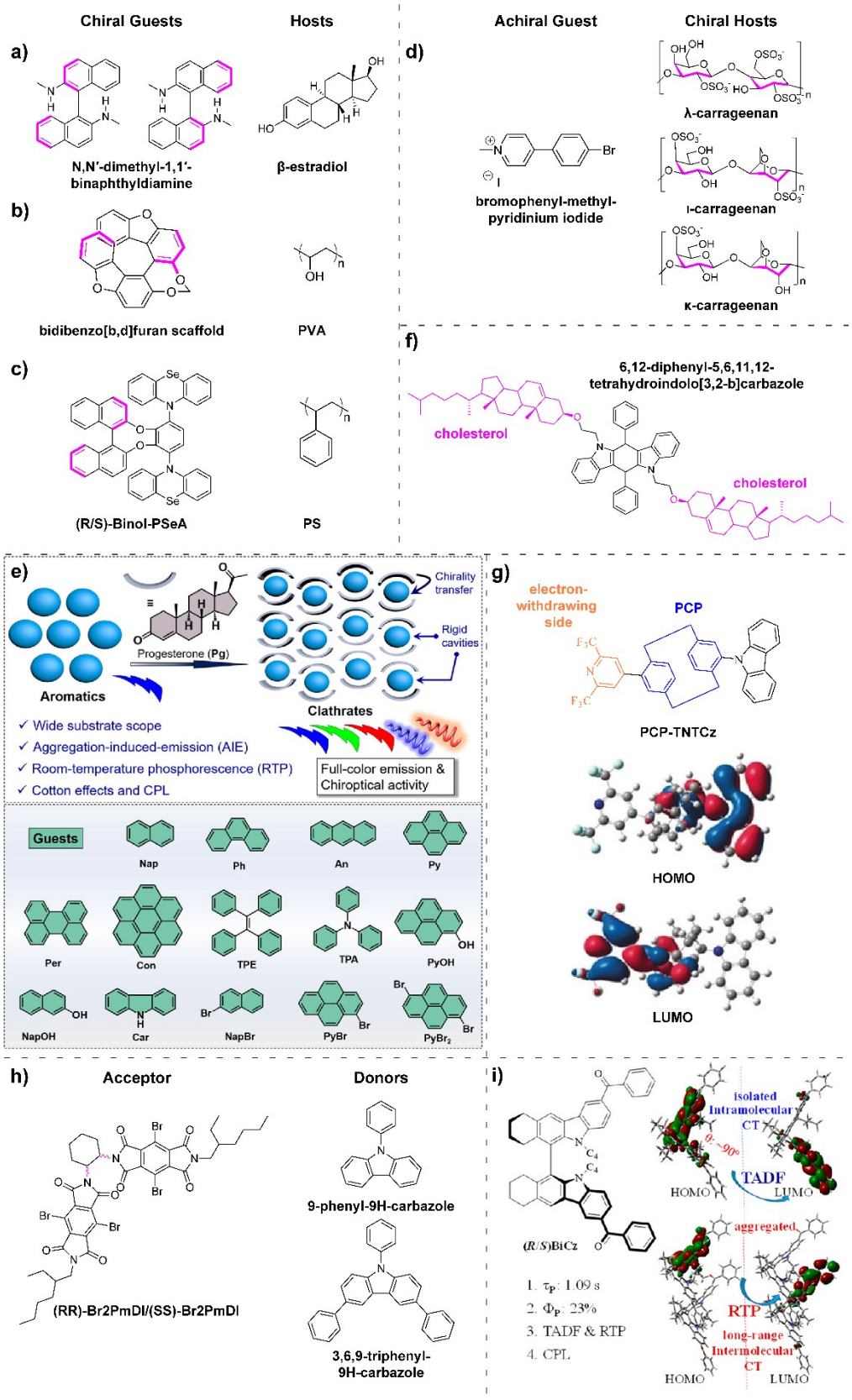

View Article Online
DOI: 10.1039/D6TC00103J

Fig. 8: Schematic of organic RTP systems exhibiting CP RTP: (a) the host and guest reported by Hirata and Vacha,[123] (b) a chiral phosphor guest and a PVA host, (c) chiral perturbation approach-based host-guest system, (d) an achiral phosphor and chiral polysaccharide matrices, (e) chirality transfer between progesterone and a range of aromatic guest molecules (Reprinted with permission from ref. [124]. Copyright 2022 American Chemical Society.), (f) chiral cholesterol groups (pink) and a Ben-2H centre, (g) HOMO-LUMO distribution of PCP-TNTCz (reproduced with permission[125]), (h) chiral bis-chromophoric pyromellitic diimides (acceptors) and achiral phenyl carbazole derivatives (donors), and (i) (R/S)-octahydro-binaphthyl-based BiCz molecule including its chirality and RTP properties (Reprinted with permission from ref. [126]. Copyright 2022 American Chemical Society.)

The integration of chiral chromophores as guests into rigid hosts is a facile strategy to achieve both RTP and intrinsically left/right-handed CP phosphorescence.[30,121,127] For instance, a pioneering study by Hirata and Vacha (Figure 8a) examined enantiomers of binaphthyl compounds doped into a hydroxylated steroid matrix leading to yellow persistent RTP in air with τ_p and ϕ_p of 0.67 s and 2.3%, respectively.[123] Additionally, the obtained $|g_{lum}|$ for the CP RTP was 2.3×10^{-3}. More recently, PVA doped by a scaffold of bidibenzo[b,d]furan (Figure 8b) led to the treated films exhibiting a ϕ_p of 14.8 %, $|g_{lum}|$ of 0.12, and τ_p of 564.5 ms under ambient conditions.[128] Similarly, integrating a chiral phosphor intro a PS matrix led to a $|g_{lum}|$ up to 9.32×10^{-3}, and ϕ_p and τ_p up to 27.0% and 40.0 ms, respectively, as well as different colours based on condition (Figure 8c).[129] However, some studies have observed decreasing phosphorescence intensity and τ_p with increasing dopant concentration, suggesting quenching due to aggregation.[130]

Chiral systems can be achieved by incorporating chiral chromophores or by copolymerizing chiral monomers.[131] Alternatively, some studies have shown that a chirality transfer can be achieved by integrating achiral phosphors into a chiral centre of a polymeric chain.[132] For example, a recent study integrated the achiral cationic phosphor bromophenyl-methyl-pyridinium iodide (PYI) into aqueous solutions of chiral anionic polysaccharides λ-carrageenan (λ-Car), ι-carrageenan (ι-Car), and κ-carrageenan (κ-Car) (Figure 8d).[133] These polysaccharides not only provide the rigid matrix for enhanced RTP, but have multiple chiral sites to achieve CP RTP. An effective chiral co-assembly led to the λ-Car@PYI suspension exhibiting CP RTP with a $|g_{lum}|$ of 2.19×10^{-3} at 580 nm, while the other two polysaccharide-based gels did not. Aside from chiral polymer matrices, other molecular matrices, like progesterone, have also shown promising CP RTP results for a wide range of achiral guest molecules (Figure 8e).[124]

The technique of integration into chiral polymers has also benefitted the development of carbon dots-based CP RTP materials.[134] These are less frequent in literature due to the insufficient molecular chirality of the organic precursors to produce CP light, as well as water solubility of some carbon dot systems making chirality transfer difficult. Nonetheless, carbon dots made from precursor materials urea and (R/S)-1,1'-binaphthyl-2,2'-diamine exhibited intrinsic CP fluorescence and CP RTP dual emission.[135] Their results showed that the obtained $|g_{lum}|$ was of the order 10^{-3} with τ_p of up to 400 ms, and when combined with achiral helical polyacetylene, the $|g_{lum}|$ increased to 0.020 at 470 nm. These results were explained by both the charge transfer excitations within the carbon dots, due to the presence of carbonyl and nitrogen groups, and the chirality transfer from the carbon dots to the achiral helical chains, thus enhancing chiroptical performance.

Aggregation-induced chirality transfer has also been reported as an alternative strategy. Fu et al. found that the chiral luminophore Ben-2Chol (Figure 8f) can self-assemble to form aggregates in solution and in thin-films, leading to a maximum $|g_{lum}|$ of 1.1×10^{-3}.[136] Additionally, its liquid phase diffused fibrous microcrystals showed inverted polarization, achieving $|g_{lum}|$ values of 6.0×10^{-3} (blue) and 1.0×10^{-3} (yellow-green) with a τ_p of 41.7 ms at 541 nm. Ye et al. recently reported a chiral ionic crystal strategy to confine isolated chromophores for enhanced CP RTP by chirality transfer.[137] They employed 2,2'-bipyridine-5,5'-dicarboxylic acid as the chromophore, due to the two carboxyl groups for enhancing ISC and ease of ionization for ionic bonding, and R/S-α-methylbenzylamines as the counterions. Results showed that the τ_p relative to maximum emission and the ϕ_p were 22.19 and 22.81 ms and 43.2% and 39.2%, for the R and S enantiomers, respectively, further confirming the rigidity offered by the ionic bonding, while obtaining $|g_{lum}|$ values of the order of 10^{-1}.

Another key strategy explored in recent years is that of charge transfer mechanisms such as through-space charge transfer (TSCT).[125] One of the first reports of this mechanism was that by Liang et al. who observed TSCT based on a [2.2]paracyclophane (PCP) centre leading to CP RTP with $|g_{lum}|$ values as high as -1.2×10^{-2} in toluene, and a τ_p of 313.59 ms.[125] The TSCT mechanism could be established via the HOMO-LUMO distribution within the molecule, as it was observed that the HOMO was distributed on the carbazole moieties and adjacent phenyl rings and the LUMO was distributed on the electron-withdrawing moieties and the connected phenyl rings (Figure 8g). More recently, this phenomenon was observed when heavy atom-substituted bis-chromophoric pyromellitic diimides and achiral phenyl carbazole derivatives were combined, leading to a CP RTP ϕ_p of around 46% and a high $|g_{lum}|$ of around 3.6×10^{-2} (Figure 8h).[138]

Song et al. designed (R/S)-octahydro-binaphthyl-based bicarbazoles (BiCz) (Figure 8i).[126] This design relied on a few key factors: (1) the carbazoles' axial chirality and twisted helical structure facilitating CP luminescence; (2) the intramolecular charge transfer from one carbazole unit to another; (3) the intermolecular charge transfers in the aggregated state; (4) the steric hindrance decreasing exciton annihilation; and (5) the $n-\pi^*$ aromatic ketone groups facilitating the El-Sayed rule for RTP. The material exhibited a Φ_p of 23% and a promising τ_p of 1.09 s.

3. Applications

Added functionalities to RTP materials widens the scope of their applications. One of the major applications of functional RTP materials discussed herein is X-ray scintillation. Organic scintillators that exhibit efficient X-ray excited

photoluminescence are incredible materials for medical diagnostics and security screening applications.[109] For instance, the halogen-atom containing organic phosphor-based scintillators by Wang et al. exhibited an X-ray detection limit of 33 nGy/s which is 167 times lower than the standard dosage for an X-ray medical examination, exemplifying great potential for RTP materials in the field of medicine.[105]

Some recent studies that have proven the applicability of scintillating RTP materials include that of Sun et al. who designed a co-polymer with a triazine moiety acceptor and 9,9-dimethylacridan donor, which was doped within a PMMA matrix for high-resolution X-ray imaging applications.[139] Their results demonstrate the versatility of RTP scintillators, as one of their RTP-PMMA films showed low detection limits of 62.27 nGy/s, featuring well-balanced radiative transition channels. Moreover, the material achieved a high spatial resolution of 20 line pairs/mm, with high-resolution X-ray images obtained at various temperatures, further supporting the applicability in X-ray imaging and radiography. Similarly, TPA-DCPP-doped oIPhCz on polydimethylsiloxane (PDMS) films fabricated on glass sheets showed flexibility as well as colour-tuneable X-ray scintillating properties.[113] In 2022, Wei et al. drop-casted a polymer methanol solution onto a quartz plate to form a transparent scintillator screen for X-ray imaging with a resolution of 8.7 line pairs/mm.[106] Additionally, many of the previously discussed RTP scintillators can be applied to large-area fabrication and flexible X-ray imaging.[108,110,140]

Another key application of functional RTP materials are OLEDs, particularly in the context of CP RTP.[141–143] This can be attributed to the concept that OLEDs with direct generation of CP light offer lower energy losses, where anti-glare layers made using CP filters can reduce light transmission from conventional unpolarized OLEDs.[144,145] Given that CP is generally applicable to 3D display technology, CP RTP may enable future 3D OLED displays.

Overall, integration of RTP properties may enhance the efficiency of OLED devices. This is because electrical injection of electrons results in a statistical ratio of 25% singlet excitons and 75% triplet excitons. Given that fluorescence is generated only from singlet states, enabling phosphorescent deexcitation pathways considerably increases internal quantum efficiency.[30,146] For instance, a polycyclic donor-acceptor framework consisting of benzenedithiol, binaphthol and dicyanobenzene was constructed.[147] This system led to simultaneous blue TADF and yellow RTP that contributed to single-molecule white OLED emission. The design also served as one of the first single chiral molecule-based white OLED material. A similar dual emission was also recently exhibited by a CP-OLED made from 9,9-Dimethyl-10-phenyl-9,10-dihydroacridine that exhibited a high maximum EQE of 32.44%.[148]

Flexible OLED materials comprise another class of materials with great promise in flexible electronics. Qiu et al. designed a flexible 4,6-di(thianthren-1-yl)pyrimidine (mTEPm) molecule exhibiting RTP, that integrated the heavy atom effect and could undergo twist conformations. The structure exhibited a maximum external quantum efficiency (EQE) of 7.98%.[149]

Data security is another field where RTP materials may be useful; by introducing additional functionalities such as flexibility, the materials can integrate encrypted information with 3D spatial dependence due to the materials' anisotropic optical properties and mechanical modulation capabilities.[33] Anticounterfeiting applications of flexible RTP materials have been reported multiple times in literature.[37,46,150] For instance, Zhao et al. designed a dynamic anticounterfeiting electrocardiogram (ECG) display using GCP-4 (Figure 9).[58] An obscured ECG pattern was printed onto an unstressed GCP film to block UV excitations. However, once the film was uniaxially stretched, the ECG could return to its standard form, showing the true encoded information. This shows how these RTP polymers could be used for both static and dynamic anticounterfeiting applications. Similarly, recent studies have also considered dynamic/stimuli-responsive materials.[73,151–154] For instance, carbon quantum dots (CQDs) of histidine or 2,4,6-triaminopyrimidine led to water and heat–responsive RTP, as well as time-resolved multi-colour dynamic anti-counterfeiting properties, realizing efficient information encryption using various stimuli.[155]

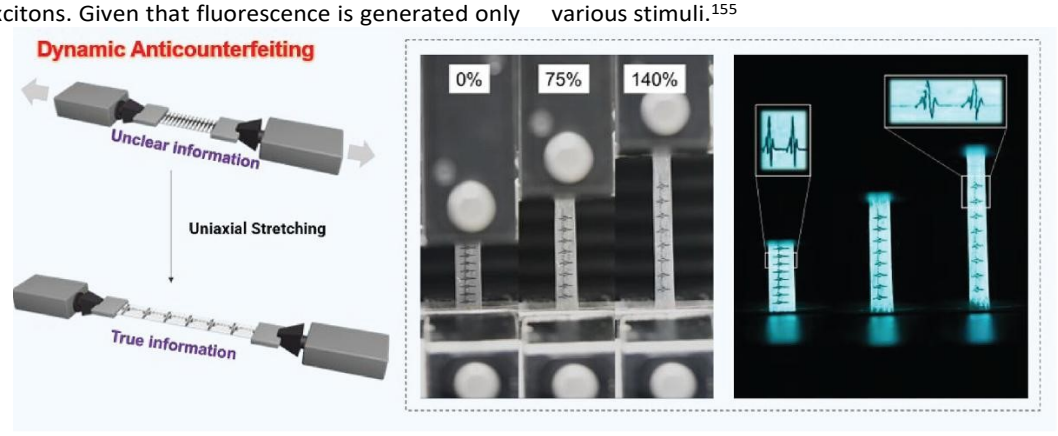

Fig. 9: Schematic of dynamic counterfeiting displays by GCP-4 (Reprinted with permission from ref. [58]. Copyright 2023 American Chemical Society.)

RTP-based sensing is another application currently discussed in literature. Wei et al. showed how ionogels can be applied to motion sensing, as they accurately and reversibly respond to different strains ranging from 10% to 100%, as a result of the gels' intrinsic elasticity.[48] The strain could be measured through the electrical output of the device, as the

two were strongly and linearly correlated, with a correlation coefficient of 0.995. Temperature sensing has also been demonstrated in donor-acceptor composites based on tetra-donor-substituted corannulenes with phenylene bridges.[156] The variations in conformational energies of each molecule's triplet states manifested in changes in the ratio of multiple phosphorescence yields as temperature varied. There are also instances where thermochromic CP RTP materials have been reported, which could potentially be used in similar applications.[157]

4. Discussion and Future Outlook

New applications are driving the increasing demand for RTP materials with additional functionalities, such as inherent flexibility, stimulus-responsiveness, and other transductive functions. Polymeric RTP materials are currently more prevalent in literature than small molecules and other systems. This may be associated with certain intrinsic properties, such as higher flexibility and tunability, which is crucial to many functionalities. Additionally, polymer systems tend to be associated with more facile synthesis, greater thermal stability, and economic viability to scale up, with their proven track record motivating researchers to continue on this path.[5]

Recent research has extended functional RTP systems to exhibit good operational stability in various environments, further realizing applications of these materials. For instance, many dynamic RTP systems have been reported to show stable performances across multiple cycles of exposing to and removing specific stimuli.[158,159]

Strategic material choice plays a key role in enhanced stability. As Zhang et al. find, improved intermolecular interactions between host and guest molecules, as was observed in their modified vanilla-doped PVA systems, can lead to high τ_p and ϕ_p.[159] However, while PVA or polyacrylamide are common matrices for host-guest doping, phosphorescent intensities and τ_p of such host-guest systems may be easily prone to quenching by water/humidity, making them less applicable outside a laboratory setting.[160] Hence, opting for hydrophobic matrices or matrices that can effectively shield phosphors from water is an important direction to undertake.

Miao et al. recently reported a host-guest doping strategy that led to ultralong photoactivated RTP with τ_p of 5.82 s, achieved by doping polyvinyl butyral resin (contains polyvinyl butyral, PVA and polyvinyl acetate) with rigid triphenylene derivatives.[160] Aside from exhibiting a tensile modulus of 2.08 GPa and elongation at break of 99%, their doped system also exhibited excellent robustness with respect to lifetimes when immersed in different water samples for long durations (rain water, tap water, lake water), allowing for the system to potentially be applied as stable phosphorescent labels in outdoor environments. Such water-resistant/humidity-resistant systems have been increasingly reported, with common strategies involving strong and robust polymeric networks.[59,161]

A recent study reported that the afterglow of a flexible polymer system was around 24 hours, which is close to 4 orders of magnitude greater than typical organic RTP systems.[162] The design relied on strong intermolecular interactions between a polyester matrix and aromatic chromophores leading to stable phosphorescent intensities even when the sample was in air or in water for 2 months, further asserting the importance of matrix choice and modulating matrix-chromophore interactions.

Alternatively, opting for carbon dot-based materials could facilitate greater operational stability of certain RTP systems. For instance, Zheng et al. reported that their carbon dot-based composite RTP materials showed consistent phosphorescent intensities despite being immersed in aqueous solution between 1 and 72 hours, indicating the anti-quenching properties of the material.[163] Additionally, thermogravimetric analysis exhibited high thermal stability – another key aspect for RTP applicability.

In relation to quenching by atmospheric oxygen, opting for matrices that have low permeability to oxygen increases overall stability. However, in scenarios where oxygen permeability may be high, photoactivated RTP could be a potential direction to undertake.[164,165] This was the strategy employed by Zhou et al. who in-situ polymerized lignin, a chromophoric biomolecule, into one of two matrices: PLA or PVA.[28] These matrices had oxygen permeability values of 41918.58 $cm^3mm^{-2}Pa^{-1}day^{-1}$ and 1.52 $cm^3mm^{-2}Pa^{-1}day^{-1}$, respectively, allowing for RTP to be easily observed in PVA-lignin under immediate UV excitation. However, upon prolonged exposure of PLA-lignin to UV, persistent afterglow was observed, attributable to the residual oxygen being converted into excited singlet state O_2 with the aid of lignin's excited triplet state, such that eventually, RTP of the lignin moiety in PLA-Lig was activated.

While most of the studies discussed herein focus on materials exhibiting solely RTP, some novel dual emission materials combine RTP with other emissive mechanisms, such as TADF. Given that these emissive phenomena vary in terms of their lifetimes and intensities, possessing multi-emissive properties enables the design of wide-range sensors in dynamic systems. These dual emission materials allow for the selection of different time windows and wavelengths, proving beneficial, as well, for more versatile and customizable OLED displays.[166,167] In an early study by Zhan et al. two multi-functional emitters were examined which combined RTP, TADF, aggregate-induced emission, and mechanoluminescence.[168] Another interesting example was reported by Dong et al., who demonstrated the temperature-adaptive scintillating properties of three novel 4,6-di(thianthren-1-yl)pyrimidine derivatives.[169] These molecules exhibited both phosphorescence and TADF dual emissions, as well as effective X-ray scintillation. This behaviour is attributed to the small energy gap between the singlet and triplet states and the presence of heavy atoms which allows for dual photoemission triggered by both UV and X-rays. Above room temperature, the reverse ISC processes were faster than radiative decay, resulting in TADF domination. Likewise, reduced temperatures resulted in accelerated triplet exciton decay and a higher degree of phosphorescence. As such, the nature of the emission would be dependent on the temperature of the device.

Aside from this, recent studies have explored multifunctional materials, such as combined flexibility and scintillation and/or stimuli-responsive materials. For instance, leveraging a dynamic hydrogen-bonding strategy can allow for the design of RTP materials that are both dynamic and malleable, as was achieved by incorporating naphthylamide-grafted polydimethylsiloxane into a polyacrylic acid matrix.[170] Another seminal study explored CP RTP materials, made from anionic cellulose derivatives, that showed dynamic changes when exposed to varying humidities, temperatures, and pH, while also exhibiting excitation-dependence, time-dependence, and visible-light excitation. As a result, these materials could be applied for advanced data encryption, revealing information that is stimuli specific.[171] Nonetheless, there is still limited research on materials that exhibit multi-model responsiveness, or materials that are both scintillating or circularly polarizing and flexible, which could be applied to X-ray bioimaging or analytical instrumentation.[25] For instance, flexible CP RTP materials can diversify applications of highly efficient OLED display technology. Similarly, flexible X-ray scintillators can facilitate precise 3D X-ray imaging of non-planar objects that are otherwise vulnerable to producing distorted images when examined via conventional rigid X-ray scintillators.[172,173] From an applications standpoint, flexibility allows for wearable radiation detectors and conformal X-ray bioimaging.[173]

In some cases, one must consider balancing potentially contradicting aspects of materials design. For example, designing flexible materials and devices comes at the expense of rigidity of the material, which may increase non-radiative transitions and reduce RTP intensity. As Deng et al. report, conventional dynamic RTP hydrogels that would be of great benefit for phosphorescent skins, for instance, are vulnerable to performance trade-off, as improved flexibility could lead to lower τ_p and vice versa.[174] Hence, they opted for a crystalline confinement strategy that allowed for balancing this trade-off effectively, and can be an effective strategy for dynamic RTP hydrogels moving forward.[174]

Another consideration is mechanochromic and thermochromic properties. For example, this can be leveraged for sensing applications, but it may hinder other applications such as flexible anticounterfeiting systems. Here, RTP behaviour must be efficaciously tuned to meet security-related demands and not be easily affected by variations in temperature or strain. In this scenario, polymeric design strategies, which tend to offer better flexibility and even "turn-on" RTP behaviour, could be a promising direction.

Although blue phosphorescence is crucial for full-colour displays and white light generation, there are few blue RTP materials which exhibit long τ_p and high ϕ_p.[175] The challenge lies in the increased probability of energy losses and the reliance on unstable high-energy triplet excitons. A very recent study employed a positional isomerism approach, integrating pinacol boronate ester groups at various positions of carbazoles and doping these moieties into PVA.[175] The systems showed visible blue RTP with tuneable τ_p from 3.96 s to 5.20 s and high ϕ_p from 17.94 to 26.95%. This research paves the way for designing functional blue RTP materials in the future.

From a commercialization standpoint, scaling up functional RTP systems requires design strategies that are cheap and reliable on large scales. In this regard, extensive consideration of the choice of raw material and synthesis methodologies plays a fundamental role. In comparison to their inorganic predecessors, organic RTP materials have inherent advantages in functional RTP behaviour such as enhanced flexibility, low-temperature processing requirements, and greater availability of raw materials that are typically less toxic.[103] As previously mentioned, polymeric functional RTP materials may therefore be the key to upscaling RTP material production, given their high processability, low costs, and general biocompatibility.[176] Within these polymeric materials, opting for simpler synthetic routes, such as click reactions, can further increase reaction rates, and even be solution-processed in green solvents, such that RTP materials can be produced in a facile manner and in larger scales.[60,177]

We also find that across different reports on functional RTP materials, there is an apparent need for standardized reporting of the associated properties. As observed in Table 1, a significant portion of works on flexible RTP materials provide only a subjective description of their materials as "flexible", without reporting tensile strain, strength, and/or moduli. Failure to quantify such functional parameters prevents objective comparison between materials. Hence, it is vital that future reports provide a range of quantitative measures, such as g_{lum} values for CP RTP, tensile strains for flexible systems, or detection limits for X-ray scintillators, in addition to photophysical properties.

Furthermore, future research can shift the development of new materials toward more biodegradable materials or biomaterials.[25] This would not only facilitate the biocompatibility of functional materials for use in fields like medicine, but also encourage sustainability and closed-loop recyclability. For instance, a recent study by Cao et al. took advantage of the phosphorescence-active biomolecule lignosulfonate, which is intrinsically achiral, co-assembled with chiral cellulose nanocrystals.[178] This resulted in CP RTP with a $|g_{lum}|$ of 0.21 and a τ_p of 103 ms, constituting an important precedent toward biomaterial-based RTP. Similarly, the aforementioned cellulose-based multi-model responsive CP RTP system exhibited good biodegradability and biocompatibility.[171]

Finally, while purely organic functional RTP materials pose great advantages, their RTP parameters (including τ_p and ϕ_p) have yet to meet those of their inorganic counterparts. For instance, as stated by Dou et al., polymeric RTP systems that exhibit both Φ_p more than 10% and τ_p more than 1 s are rarely reported, especially in solution.[15] This requires further development of new and existing design strategies, with biomimetic design as a potentially viable approach.

Author contributions

N. G. and D. C. conceived of the topic for this highlight. D. C. wrote the original draft. D. C, N. G, F. A, and S. M. P reviewed and edited the manuscript.

Conflicts of interest

There are no conflicts to declare.

Data availability

No primary research results, software or code have been included and no new data were generated or analysed as part of this review.

Acknowledgements

This work was supported by the National University of Singapore Presidential Young Professorship (A-0010035-00-00; A-0010035-01-00), the Ministry of Education, Singapore, under the Academic Research Fund Tier 1 (A-8002904-00-00).

References

1 Y. Yang, Q. Li and Z. Li, *Mater. Chem. Front.*, 2025, **9**, 744–753.
2 X. Luo, B. Tian, Y. Zhai, H. Guo, S. Liu, J. Li, S. Li, T. D. James and Z. Chen, *Nat. Rev. Chem.*, 2023, **7**, 800–812.
3 X. Zhang, J. Liu, B. Chen, X. He, X. Li, P. Wei, P. F. Gao, G. Zhang, J. W. Y. Lam and B. Z. Tang, *Matter*, 2022, **5**, 3499–3512.
4 M. He, C. Ding, H. Guo and Q. Li, *Responsive Mater.*, 2024, DOI:10.1002/rpm.20240014.
5 H. Wang, N. Gan, L. Han, Z. Meng and Z. An, in *Optical and Optoelectronic Polymers*, Royal Society of Chemistry, 2024, pp. 236–310.
6 N. Gan, X. Zou, Y. Zhang, L. Gu and Z. An, *Appl. Phys. Rev.*, 2023, DOI:10.1063/5.0140824.
7 Kenry, C. Chen and B. Liu, *Nat. Commun.*, 2019, **10**, 2111.
8 Y. Patil, C. Demangeat and L. Favereau, *Chirality*, 2023, **35**, 390–410.
9 W. Zhao, Z. He and B. Z. Tang, *Nat. Rev. Mater.*, 2020, **5**, 869–885.
10 W. Zhao, Z. He, J. W. Y. Lam, Q. Peng, H. Ma, Z. Shuai, G. Bai, J. Hao and B. Z. Tang, *Chem*, 2016, **1**, 592–602.
11 G. Zhang, J. Chen, S. J. Payne, S. E. Kooi, J. N. Demas and C. L. Fraser, *J. Am. Chem. Soc.*, 2007, **129**, 8942–8943.
12 J. Guo, C. Yang and Y. Zhao, *Acc. Chem. Res.*, 2022, **55**, 1160–1170.
13 H. Zheng, Z. Zhang, S. Cai, Z. An and W. Huang, *Adv. Mater.*, 2024, DOI:10.1002/adma.202311922.
14 S. K. Lower and M. A. El-Sayed, *Chem. Rev.*, 1966, **66**, 199–241.
15 X. Dou, X. Wang, X. Xie, J. Zhang, Y. Li and B. Tang, *Adv. Funct. Mater.*, 2024, DOI:10.1002/adfm.202314069.
16 Z. Yan, X. Lin, S. Sun, X. Ma and H. Tian, *Angew. Chemie Int. Ed.*, 2021, **60**, 19735–19739.
17 Y. He, J. Wang, Q. Li, S. Qu, C. Zhou, C. Yin, H. Ma, H. Shi, Z. Meng and Z. An, *Adv. Opt. Mater.*, 2023, DOI:10.1002/adom.202201641.
18 H. Zhang, Y. Guo, Z. Wu, Y. Wang, Y. Sun, X. Feng, H. Wang and G. Zhao, *J. Lumin.*, 2021, **232**, 117864.
19 D. Ding, X. Xu, F. Li, A. Saparbaev, E. Zakhidov and M. Sun, *Small*, 2025, DOI:10.1002/smll.202503142.
20 S. Jena, J. Eyyathiyil, S. K. Behera, M. Kitahara, Y. Imai and P. Thilagar, *Chem. Sci.*, 2022, **13**, 5893–5901.
21 B. Ding, X. Ma and H. Tian, *Accounts Mater. Res.*, 2023, **4**, 827–838.
22 S. Datta and J. Xu, *ACS Appl. Bio Mater.*, 2023, **6**, 4572–4585.
23 T. Wang, Y. Fu, J. Wang, G. Li, J. Sun, Q. Liu, Y. Zhao, Z. Zhang, Z. Wang, S. Wang, Z. Zheng, Y. Wang and Y. Lu, *Adv. Mater.*, 2025, DOI:10.1002/adma.202512659.
24 Q. Zhou, C. Yang and Y. Zhao, *Chem*, 2023, **9**, 2446–2480.
25 W. Gao, D. Li, H. Feng and Z. Su, *J. Mater. Chem. C*, 2025, **13**, 13607–13619.
26 T. Cai, Y.-Z. Yan, J. Jung, J. Han, E. Yeom, Y. Im, T. Lee, D. Peng, Y. Liu, C.-S. Ha and K. C. Kim, *Sensors Actuators A Phys.*, 2021, **332**, 113205.
27 T. Cai, Y.-Z. Yan, Y. Park, T. Lee, D. Peng, Y. Liu, C.-S. Ha and K. C. Kim, *ACS Appl. Polym. Mater.*, 2021, **3**, 2461–2469.
28 J. Zhou, B. Tian, Y. Zhai, M. Wang, S. Liu, J. Li, S. Li, T. D. James and Z. Chen, *Nat. Commun.*, 2024, **15**, 7198.
29 B. Huang, Y. Zhang, T. Wang, B. Mei, P. Sun, J. Shi, B. Tong, Z. Liu, Z. Cai and Y. Dong, *Mater. Chem. Front.*, 2025, **9**, 3495–3504.
30 X. Zou, N. Gan, Y. Gao, L. Gu and W. Huang, *Angew. Chemie Int. Ed.*, 2025, DOI:10.1002/anie.202417906.
31 H. Li, Z. Tang, Z. Liu and C. Zhi, *Joule*, 2019, **3**, 613–619.
32 E. Dauzon, X. Sallenave, C. Plesse, F. Goubard, A. Amassian and T. D. Anthopoulos, *Adv. Mater.*, 2021, DOI:10.1002/adma.202101469.
33 X. Wei, J. Ye, L. Shi and R. Jia, *Adv. Opt. Mater.*, 2025, DOI:10.1002/adom.202500106.
34 J. Wei, J. Hu, M. Zhu, J. Wu, M. Xiao, Y. Wang, Y. Zhou, S. Liu, Y. Ma and Q. Zhao, *Laser Photon. Rev.*, 2025, DOI:10.1002/lpor.202400971.
35 Y. Zhu, H. Wu, M. Pan, L. Ma and Y. Wang, *Chem. Eng. J.*, 2025, **519**, 165087.
36 Y. Zhu, M. Pan, L. Ma and Y. Wang, *Chem. Eng. J.*, 2025, **505**, 159245.
37 X. Yang, N. Li, B. Wang, P. Chen, S. Ma, Y. Deng, S. Lü and Y. Tang, *Angew. Chemie Int. Ed.*, 2025, DOI:10.1002/anie.202419114.
38 F. Guo, Y. Chen, C. Li, X. Wang, Q. Li, M. He, H. Hou and C. Yang, *Adv. Funct. Mater.*, 2025, DOI:10.1002/adfm.202416465.
39 N. Gan, X. Zou, Z. Qian, A. Lv, L. Wang, H. Ma, H.-J. Qian, L. Gu, Z. An and W. Huang, *Nat. Commun.*, 2024, **15**, 4113.
40 Y. Xia, C. Zhu, F. Cao, Y. Shen, M. Ouyang and Y. Zhang, *Angew. Chemie Int. Ed.*, 2023, DOI:10.1002/anie.202217547.
41 Z. Lin, R. Kabe, N. Nishimura, K. Jinnai and C. Adachi, *Adv. Mater.*, 2018, DOI:10.1002/adma.201803713.
42 W. Sun, B. Shi, Z. Xia and C. Lü, *Mater. Today Chem.*, 2023, **27**, 101297.
43 W. Tao, Y. Zhou, F. Lin, H. Gao, Z. Chi and G. Liang, *Adv. Opt. Mater.*, 2022, DOI:10.1002/adom.202102449.
44 Y. Zhang, Q. Sun, L. Yue, Y. Wang, S. Cui, H. Zhang, S. Xue

and W. Yang, *Adv. Sci.*, 2022, DOI:10.1002/advs.202103402.
45 L. Yue, Q. Sun, Y. Zhang, Y. Wang, S. Cui, H. Zhang, S. Xue and W. Yang, *Chem. Eng. J.*, 2022, **433**, 134307.
46 J. Cao, J. Song, Y. Hu, F. Zhang, H. Tian and X. Ma, *ACS Mater. Lett.*, 2025, 3227–3234.
47 C. Wei, L. Bai, X. An, M. Xu, W. Liu, W. Zhang, M. Singh, K. Shen, Y. Han, L. Sun, J. Lin, Q. Zhao, Y. Zhang, Y. Yang, M. Yu, Y. Li, N. Sun, Y. Han, L. Xie, C. Ou, B. Sun, X. Ding, C. Xu, Z. An, R. Chen, H. Ling, W. Li, J. Wang and W. Huang, *Chem*, 2022, **8**, 1427–1441.
48 X. Wei, Z. Gou, J. Ye, L. H. Shi, J. Zhao, L. Yang, L. Zhang, K. Zhang and R. Jia, *Adv. Sci. (Weinheim, Baden-Wurttemberg, Ger.*, 2024, **12**, e2411229.
49 Z. Xu, Y. Huang, S. Sun, P. Wang, Z. He, H. Tian and X. Ma, *Angew. Chemie*, 2025, DOI:10.1002/ange.202518340.
50 X. Huang, Y. Zhang, G. Li, T. Wang, P. Sun, J. Shi, B. Tong, J. Zhi, Z. Li, Z. Cai and Y. Dong, *ChemPhotoChem*, 2025, DOI:10.1002/cptc.202400315.
51 H. Chen, X. Ma, S. Wu and H. Tian, *Angew. Chemie Int. Ed.*, 2014, **53**, 14149–14152.
52 J. Deng, H. Liu, D. Liu, L. Yu, Y. Bai, W. Xie, T. Li, C. Wang, Y. Lian and H. Wang, *Adv. Funct. Mater.*, 2024, DOI:10.1002/adfm.202308420.
53 J. Xiao, J. Deng, X. Wang, H. Ho, C. Bai, Y. Bai and H. Wang, *Small*, 2024, DOI:10.1002/smll.202405615.
54 H. Ju, H. Zhang, L. X. Hou, M. Zuo, M. Du, F. Huang, Q. Zheng and Z. L. Wu, *J. Am. Chem. Soc.*, 2023, **145**, 3763–3773.
55 W. Xie, J. Deng, Y. Cai, Y. Wang, S. He, Y. Bai, J. Xiao, X. Zhong, J. Jiang and H. Wang, *Adv. Funct. Mater.*, 2025, DOI:10.1002/adfm.202504411.
56 Y. Cao, D. Wang, Y. Zhang, G. Li, C. Gao, W. Li, X. Chen, X. Chen, P. Sun, Y. Dong, Z. Cai and Z. He, *Angew. Chemie Int. Ed.*, 2024, DOI:10.1002/anie.202401331.
57 X. Ma, C. Xu, J. Wang and H. Tian, *Angew. Chemie Int. Ed.*, 2018, **57**, 10854–10858.
58 R. Zhao, C. Wang, K. Huang, L. Li, W. Fan, Q. Zhu, H. Ma, X. Wang, Z. Wang and W. Huang, *J. Am. Chem. Soc.*, 2023, **145**, 26532–26539.
59 M. Chen, B. Liu, J. Ren, C. Zhang, Z. Ren and Z. Guan, *Adv. Mater.*, 2025, DOI:10.1002/adma.202504825.
60 R. Tian, S.-M. Xu, Q. Xu and C. Lu, *Sci. Adv.*, 2020, DOI:10.1126/sciadv.aaz6107.
61 X. Yang, Y. Dong, S. Ma, J. Ren, N. Li and S. Lü, *Chem. Eng. J.*, 2023, **462**, 142198.
62 R. Tian, S. Gao, K. Li and C. Lu, *Nat. Commun.*, 2023, **14**, 4720.
63 Y. Zhang, Y. Chen, J. Li, S. Liu and Y. Liu, *Adv. Sci.*, 2024, DOI:10.1002/advs.202307777.
64 P. Chen, H. Qie, X. Yang, S. Ma, Z. Wang, N. Li, Y. Deng, F. Bian and S. Lü, *Adv. Funct. Mater.*, 2025, DOI:10.1002/adfm.202416430.
65 W. Ji, Y. Zhao, Y. Zhu, L. Ma and Y. Wang, *Dye. Pigment.*, 2025, **240**, 112852.
66 K. Wang, L. Qu and C. Yang, *Small*, 2023, DOI:10.1002/smll.202206429.
67 X. Zhang, J. You, J. Zhang, C. Yin, Y. Wang, R. Li and J. Zhang, *CCS Chem.*, 2023, **5**, 2140–2151.
68 J. Zhou, D. Liu, L. Li, M. Qi, G. Yin and T. Chen, *Chinese Chem. Lett.*, 2024, **35**, 109929.
69 C. Zhang, X. Jiang, C. Wang, Z. Liu, B. Xu and W. Tian, *Smart Mol.*, 2025, DOI:10.1002/smo.20240054.
70 H. Sun, S. Shen and L. Zhu, *ACS Mater. Lett.*, 2022, **4**, 1599–1615.
71 R. Gavale, S. K. Pandit and R. Misra, *Chem. – An Asian J.*, 2025, DOI:10.1002/asia.202401893.
72 L. Huang, C. Qian and Z. Ma, *Chem. – A Eur. J.*, 2020, **26**, 11914–11930.
73 J. Guo, C. Hu, J. Liu, Y. Wang and L. Ma, *Dye. Pigment.*, 2024, **221**, 111760.
74 Y. Takewaki, T. Ogawa and Y. Tani, *Front. Chem.*, 2022, DOI:10.3389/fchem.2021.812593.
75 J. Yang, X. Gao, Z. Xie, Y. Gong, M. Fang, Q. Peng, Z. Chi and Z. Li, *Angew. Chemie Int. Ed.*, 2017, **56**, 15299–15303.
76 W. Luo, Y. Zhang, Y. Gong, Q. Zhou, Y. Zhang and W. Yuan, *Chinese Chem. Lett.*, 2018, **29**, 1533–1536.
77 F. Nie, B. Zhou and D. Yan, *Chem. Eng. J.*, 2023, **453**, 139806.
78 J. Guo, J. Liu, Y. Zhao, Y. Wang, L. Ma and J. Jiang, *Spectrochim. Acta Part A Mol. Biomol. Spectrosc.*, 2024, **317**, 124449.
79 Y. Gong, G. Chen, Q. Peng, W. Z. Yuan, Y. Xie, S. Li, Y. Zhang and B. Z. Tang, *Adv. Mater.*, 2015, **27**, 6195–6201.
80 H. Huang, M. Liu, X. Qiu, J. Qian, W. Dai, Y. Lei, Q. Ding, H. Wu and X. Huang, *J. Mater. Chem. C*, 2025, **13**, 2947–2955.
81 S. Li, Y. Xie, A. Li, X. Li, W. Che, J. Wang, H. Shi and Z. Li, *Sci. China Mater.*, 2021, **64**, 2813–2823.
82 Y. Tani, M. Terasaki, M. Komura and T. Ogawa, *J. Mater. Chem. C*, 2019, **7**, 11926–11931.
83 Y. Zhuang, X. Ren, X. Che, S. Liu, W. Huang and Q. Zhao, *Adv. Photonics*, 2020, DOI:10.1117/1.AP.3.1.014001.
84 L. Gu, H. Shi, M. Gu, K. Ling, H. Ma, S. Cai, L. Song, C. Ma, H. Li, G. Xing, X. Hang, J. Li, Y. Gao, W. Yao, Z. Shuai, Z. An, X. Liu and W. Huang, *Angew. Chemie Int. Ed.*, 2018, **57**, 8425–8431.
85 Y. Sun, Y. Shu, L. Zheng, Y. Song, B. Huang, X. Xu, H. Chen, J. Chang and P. Xin, *Chem. Sci.*, 2025, **16**, 17812–17819.
86 L. Gu, H. Shi, L. Bian, M. Gu, K. Ling, X. Wang, H. Ma, S. Cai, W. Ning, L. Fu, H. Wang, S. Wang, Y. Gao, W. Yao, F. Huo, Y. Tao, Z. An, X. Liu and W. Huang, *Nat. Photonics*, 2019, **13**, 406–411.
87 D. Li, J. Yang, M. Fang, B. Z. Tang and Z. Li, *Sci. Adv.*, 2022, DOI:10.1126/sciadv.abl8392.
88 Z. Wang, L. Qu, L. Gao, X. Zheng, Y. Zheng, Y. Zhu, J. Xia, Y. Zhang, C. Wang, Y. Li and C. Yang, *Adv. Opt. Mater.*, 2022, DOI:10.1002/adom.202200481.
89 H. Jin, X. Zhang, Z. Ma, C. Qian, X. Fu, Z. Li, M. Chen, Y. Guan and Z. Ma, *J. Mater. Chem. C*, 2023, **11**, 11571–11579.
90 Y. Wang, J. Yang, M. Fang, Y. Gong, J. Ren, L. Tu, B. Z. Tang and Z. Li, *Adv. Funct. Mater.*, 2021, DOI:10.1002/adfm.202101719.
91 J. Yang, X. Zhen, B. Wang, X. Gao, Z. Ren, J. Wang, Y. Xie, J.

Li, Q. Peng, K. Pu and Z. Li, *Nat. Commun.*, 2018, **9**, 840.

92 Y. Su, S. Z. F. Phua, Y. Li, X. Zhou, D. Jana, G. Liu, W. Q. Lim, W. K. Ong, C. Yang and Y. Zhao, *Sci. Adv.*, 2018, DOI:10.1126/sciadv.aas9732.

93 Y. Zhang, L. Gao, X. Zheng, Z. Wang, C. Yang, H. Tang, L. Qu, Y. Li and Y. Zhao, *Nat. Commun.*, 2021, **12**, 2297.

94 L. Li, D. Liu, J. Zhou, M. Qi, G. Yin and T. Chen, *Mater. Horizons*, 2024, **11**, 5895–5913.

95 Y. Xiao, J. Li, Z. Song, J. Liao, M. Shen, T. Yu and W. Huang, *J. Am. Chem. Soc.*, 2025, **147**, 20372–20380.

96 Y. Wang, J. Yang, Y. Gong, M. Fang, Z. Li and B. Z. Tang, *SmartMat*, 2020, DOI:10.1002/smm2.1006.

97 B. Xu, H. Wu, J. Chen, Z. Yang, Z. Yang, Y.-C. Wu, Y. Zhang, C. Jin, P.-Y. Lu, Z. Chi, S. Liu, J. Xu and M. Aldred, *Chem. Sci.*, 2017, **8**, 1909–1914.

98 T. Wang, Z. Hu, X. Nie, L. Huang, M. Hui, X. Sun and G. Zhang, *Nat. Commun.*, 2021, **12**, 1364.

99 Y. Wang, H. Gao, J. Yang, M. Fang, D. Ding, B. Z. Tang and Z. Li, *Adv. Mater.*, 2021, DOI:10.1002/adma.202007811.

100 D. Li, Y. Yang, J. Yang, M. Fang, B. Z. Tang and Z. Li, *Nat. Commun.*, 2022, **13**, 347.

101 Y. Wang, J. Yang, M. Fang, Y. Yu, B. Zou, L. Wang, Y. Tian, J. Cheng, B. Z. Tang and Z. Li, *Matter*, 2020, **3**, 449–463.

102 L. Tang, J. Zan, H. Peng, X. Yan, Y. Tao, D. Tian, Q. Yang, H. Li, Q. Chen, W. Huang and R. Chen, *Chem. Commun.*, 2020, **56**, 13559–13562.

103 H. Zhang, Y. Tan and S. Gong, *Chem. – A Eur. J.*, 2025, DOI:10.1002/chem.202404452.

104 L. Zhan, Y. Xu, T. Chen, Y. Tang, C. Zhong, Q. Lin, C. Yang and S. Gong, *Aggregate*, 2024, DOI:10.1002/agt2.485.

105 X. Wang, H. Shi, H. Ma, W. Ye, L. Song, J. Zan, X. Yao, X. Ou, G. Yang, Z. Zhao, M. Singh, C. Lin, H. Wang, W. Jia, Q. Wang, J. Zhi, C. Dong, X. Jiang, Y. Tang, X. Xie, Y. (Michael) Yang, J. Wang, Q. Chen, Y. Wang, H. Yang, G. Zhang, Z. An, X. Liu and W. Huang, *Nat. Photonics*, 2021, **15**, 187–192.

106 J. Wei, Y. Jiang, C. Liu, J. Duan, S. Liu, X. Liu, S. Liu, Y. Ma and Q. Zhao, *Adv. Photonics*, 2022, DOI:10.1117/1.AP.4.3.035002.

107 Y. Zhang, X. Wu, S. Liu, Y. Ma and Q. Zhao, *Chem. Commun.*, 2024, **60**, 9328–9339.

108 N. Gan, X. Zou, M. Dong, Y. Wang, X. Wang, A. Lv, Z. Song, Y. Zhang, W. Gong, Z. Zhao, Z. Wang, Z. Zhou, H. Ma, X. Liu, Q. Chen, H. Shi, H. Yang, L. Gu, Z. An and W. Huang, *Nat. Commun.*, 2022, **13**, 3995.

109 H. Chen, M. M. Lin, Y. Zhu, D. Zhang, J. Chen, Q. Wei, S. Yuan, Y. Liao, F. Chen, Y. Chen, M. M. Lin and X. Fang, *Small*, 2024, DOI:10.1002/smll.202307277.

110 M. Dong, A. Lv, X. Zou, N. Gan, C. Peng, M. Ding, X. Wang, Z. Zhou, H. Chen, H. Ma, L. Gu, Z. An and W. Huang, *Adv. Mater.*, 2024, DOI:10.1002/adma.202310663.

111 Z. Zhou, X. Wang, A. Lv, M. Ding, Z. Song, H. Ma, Z. An and W. Huang, *Adv. Mater.*, 2024, DOI:10.1002/adma.202407916.

112 Y. Wang, J. Yu, Z. Zhou, W. Zhao, Y. Wang, J. Zhao, C. Ma, Z.-Y. Lin, Y. Wu, X. Wang, H. Ma and W.-H. Zhu, *J. Am. Chem. Soc.*, 2025, **147**, 11098–11107.

113 H. Wang, C. Peng, M. Chen, Y. Xiao, T. Zhang, X. Liu, Q. Chen, T. Yu and W. Huang, *Angew. Chemie Int. Ed.*, 2024, DOI:10.1002/anie.202316190.

114 C. Dong, X. Wang, W. Gong, W. Ma, M. Zhang, J. Li, Y. Zhang, Z. Zhou, Z. Yang, S. Qu, Q. Wang, Z. Zhao, G. Yang, A. Lv, H. Ma, Q. Chen, H. Shi, Y. (Michael) Yang and Z. An, *Angew. Chemie Int. Ed.*, 2021, **60**, 27195–27200.

115 Z. Yang, J. Yao, L. Xu, W. Fan and J. Song, *Nat. Commun.*, 2024, **15**, 8870.

116 Y. Zhang, M. Chen, X. Wang, M. Lin, H. Wang, W. Li, F. Chen, Q. Liao, H. Chen, Q. Chen, M. Lin and H. Yang, *CCS Chem.*, 2024, **6**, 334–341.

117 K. Zhang, X.-Y. Zhang, Y.-Z. Chen, C.-H. Tung and L.-Z. Wu, *ACS Appl. Opt. Mater.*, 2026, **4**, 244–249.

118 L. Lian, M. Ai, D. Xiong, T. Liang, J. Zhang, M. Jia, Y. Liu, Z. Ma, X. Chen, Y. Han, Y. Tian, X. Li and Z. Shi, *Chem. Sci.*, 2025, **17**, 500–510.

119 J. Cao, M. Zhang, M. Singh, Z. An, L. Ji, H. Shi and Y. Jiang, *Front. Chem.*, 2021, DOI:10.3389/fchem.2021.781294.

120 S. Ye, S. Ji, M. Kang, L. Liu, J. Qu, J. Guo and J. Song, *Adv. Opt. Mater.*, 2025, DOI:10.1002/adom.202500940.

121 S. An, L. Gao, A. Hao and P. Xing, *ACS Nano*, 2021, **15**, 20192–20202.

122 J. Liu, X. Zhou, X. Tang, Y. Tang, J. Wu, Z. Song, H. Jiang, Y. Ma, B. Li, Y. Lu and Q. Li, *Adv. Funct. Mater.*, 2025, DOI:10.1002/adfm.202414086.

123 S. Hirata and M. Vacha, *J. Phys. Chem. Lett.*, 2016, **7**, 1539–1545.

124 L. Wang, A. Hao and P. Xing, *ACS Appl. Mater. Interfaces*, 2022, **14**, 44902–44908.

125 X. Liang, T. Liu, Z. Yan, Y. Zhou, J. Su, X. Luo, Z. Wu, Y. Wang, Y. Zheng and J. Zuo, *Angew. Chemie Int. Ed.*, 2019, **58**, 17220–17225.

126 J. Song, Y. Wang, L. Qu, L. Fang, X. Zhou, Z.-X. Xu, C. Yang, P. Wu and H. Xiang, *J. Phys. Chem. Lett.*, 2022, **13**, 5838–5844.

127 J. Liu, Z. Song, J. Wei, J. Wu, M. Wang, J. Li, Y. Ma, B. Li, Y. Lu and Q. Zhao, *Adv. Mater.*, 2024, DOI:10.1002/adma.202306834.

128 W. Huang, C. Fu, Z. Liang, K. Zhou and Z. He, *Angew. Chemie Int. Ed.*, 2022, DOI:10.1002/anie.202202977.

129 S. Fu, Y. Chen, Y. Xie and Z. Li, *Chinese J. Chem.*, 2024, **42**, 2499–2506.

130 S. Garain, S. Sarkar, B. Chandra Garain, S. K. Pati and S. J. George, *Angew. Chemie Int. Ed.*, 2022, DOI:10.1002/anie.202115773.

131 W. Gong, M. Zhou, L. Xiao, C. Fan, Y. Yuan, Y. Gong and H. Zhang, *Adv. Opt. Mater.*, 2024, DOI:10.1002/adom.202301922.

132 H. Li, H. Li, W. Wang, Y. Tao, S. Wang, Q. Yang, Y. Jiang, C. Zheng, W. Huang and R. Chen, *Angew. Chemie Int. Ed.*, 2020, **59**, 4756–4762.

133 M. Wang, Z. Shen, F. Zhang, Q. Yang, Z. Han, Y. An, H. Ma, Z. Xu, J. Liu, W. Yuan, K. Sui and Y. Zhao, *ACS Mater. Lett.*, 2025, **7**, 1171–1178.

134 S. Ma, H. Ma, K. Yang, Z. Tan, B. Zhao and J. Deng, *ACS Nano*, 2023, **17**, 6912–6921.

135 X. Gao, K. Pan, B. Zhao and J. Deng, *Adv. Funct. Mater.*,

2025, DOI:10.1002/adfm.202413569.
136 D. Fu, S. Liu and S. H. Liu, *Mater. Chem. Front.*, 2025, **9**, 2763–2769.
137 W. Ye, Z. Meng, G. Zhan, A. Lv, Y. Gao, K. Shen, H. Ma, H. Shi, W. Yao, L. Wang, W. Huang and Z. An, *Adv. Mater.*, 2024, DOI:10.1002/adma.202410073.
138 S. Garain, A. A. Kongasseri, S. M. Wagalgave, R. Konar, D. Deb, K. S. Narayan, P. K. Samanta and S. J. George, *Angew. Chemie Int. Ed.*, 2025, DOI:10.1002/anie.202501330.
139 J. Sun, M. Ding, H. Ma, X. Wang, M. Li, H. Wang, J. Du, Z. Zhou, A. Lv, H. Wang, Z. An, H. Shi and W. Huang, *Adv. Mater.*, 2025, DOI:10.1002/adma.202507058.
140 M. Zhao, P. Wan, J. Shi and L. Ji, *J. Mater. Chem. C*, 2025, **13**, 5424–5438.
141 X. Wu, C.-Y. Huang, D.-G. Chen, D. Liu, C. Wu, K.-J. Chou, B. Zhang, Y. Wang, Y. Liu, E. Y. Li, W. Zhu and P.-T. Chou, *Nat. Commun.*, 2020, **11**, 2145.
142 Y. Yang, S. Xiao, Y. Zhou, C. Shi, L. Xu, X. Liao, N. Su, N. Sun, Y.-X. Zheng, L. Ding and J. Ding, *Sci. China Mater.*, 2025, **68**, 1351–1358.
143 B. Yang, S. Yan, S. Ban, H. Ma, Y. Zhang, F. Feng and W. Huang, *Chem. Sci.*, 2025, **16**, 9393–9405.
144 M. Poncet, J. Jiménez, F. Zinna, C. Piguet, L. Di Bari, C. Botta and U. Giovanella, *Small*, 2025, DOI:10.1002/smll.202512638.
145 J. Zheng, Y. Fu, J. Wang, W. Zhang, X. Lu, H.-Q. Lin, L. Shao and J. Wang, *Nat. Commun.*, 2025, **16**, 1658.
146 B. Yang, S. Yan, S. Ban and W. Huang, *Chinese Chem. Lett.*, 2025, 110837.
147 M. Li, Z. Li, X. Peng, D. Liu, Z. Chen, W. Xie, K. Liu and S. Su, *Angew. Chemie Int. Ed.*, 2025, DOI:10.1002/anie.202420474.
148 N. Su, J. Wang, Y. Yang, Z. Yan, L. Zhou, Y. Zheng and J. Ding, *Angew. Chemie Int. Ed.*, 2025, DOI:10.1002/anie.202512717.
149 W. Qiu, X. Cai, Z. Chen, X. Wei, M. Li, Q. Gu, X. Peng, W. Xie, Y. Jiao, Y. Gan, W. Liu and S.-J. Su, *J. Phys. Chem. Lett.*, 2022, **13**, 4971–4980.
150 Y. Yang, Y. Liang, Y. Zheng, J. Li, S. Wu, H. Zhang, T. Huang, S. Luo, C. Liu, G. Shi, F. Sun, Z. Chi and B. Xu, *Angew. Chemie*, 2022, DOI:10.1002/ange.202201820.
151 H. Deng, G. Li, H. Xie, Z. Yang, Z. Mao, J. Zhao, Z. Yang, Y. Zhang and Z. Chi, *Angew. Chemie*, 2024, DOI:10.1002/ange.202317631.
152 J. Chen, J. Tan, P. Liang, C. Wu, Z. Hou, K. Shen, B. Lei, C. Hu, X. Zhang, J. Zhuang, L. Sun, Y. Liu and M. Zheng, *Small*, 2024, DOI:10.1002/smll.202306323.
153 X. Ma, T. Ye, H. Yang, G. Ling, D. Wang, J. Li, P. Gu, L. Xu, T. Sheng, F. Lin, R. Shen and Q. Zhang, *Aggregate*, 2024, DOI:10.1002/agt2.579.
154 P. Zhang, X. Chen, J. Li, L. Fang and X. Sun, *Inorg. Chem. Front.*, 2025, DOI:10.1039/D5QI01664A.
155 L. Yang, Q. Zhang, Y. Ma, H. Li, S. Sun and Y. Xu, *Chem. Eng. J.*, 2024, **490**, 151679.
156 C. Si, T. Wang, A. K. Gupta, D. B. Cordes, A. M. Z. Slawin, J. S. Siegel and E. Zysman-Colman, *Angew. Chemie*, 2023, DOI:10.1002/ange.202309718.
157 F. Nie and D. Yan, *Angew. Chemie*, 2023, DOI:10.1002/ange.202302751.
158 W.-T. Fan, Y. Chen, J. Niu, T. Su, J.-J. Li and Y. Liu, *Adv. Photonics Res.*, 2021, DOI:10.1002/adpr.202000080.
159 Y. Zhang, Z. Wang, Y. Su, Y. Zheng, W. Tang, C. Yang, H. Tang, L. Qu, Y. Li and Y. Zhao, *Research*, 2021, DOI:10.34133/2021/8096263.
160 Y. Miao, F. Lin, D. Guo, J. Chen, K. Zhang, T. Wu, H. Huang, Z. Chi and Z. Yang, *Sci. Adv.*, 2024, DOI:10.1126/sciadv.adk3354.
161 Z. Zhao, P. Zhao, S. Chen, Y. Zheng, J. Zuo and C. Li, *Angew. Chemie Int. Ed.*, 2023, DOI:10.1002/anie.202301993.
162 J. Shi, Y. Lan and G. Liang, *Matter*, 2025, DOI:10.1016/j.matt.2025.102374.
163 Y. Zheng, Q. Zhou, Y. Yang, X. Chen, C. Wang, X. Zheng, L. Gao and C. Yang, *Small*, 2022, DOI:10.1002/smll.202201223.
164 J. Liang, J. Yang, Y. Wang, M. Shan, Z. Liu, J. Ren, M. Fang and Z. Li, *Sci. China Mater.*, 2024, **67**, 2778–2788.
165 Z. Yang, H. Liu, X. Zhang, Y. Lv, Z. Fu, S. Zhao, M. Liu, S. Zhang and B. Yang, *Adv. Mater.*, 2024, DOI:10.1002/adma.202306784.
166 D. Dou, W. Liu, X. Zhou, Q. Yang, X. Tan, N. Ugur, C. Li, C. Ramanan, X. Liu, G.-J. A. H. Wetzelaer, D. Andrienko, M. Baumgarten, P. W. M. Blom and Y. Li, *Light Sci. Appl.*, 2026, **15**, 4.
167 Y. Xiong, J. Gong, J. Liu, D. Wang, H. Wu, Z. Zhao, M. Fang, Z. Li, D. Wang and B. Z. Tang, *J. Mater. Chem. C*, 2022, **10**, 10009–10016.
168 L. Zhan, Z. Chen, S. Gong, Y. Xiang, F. Ni, X. Zeng, G. Xie and C. Yang, *Angew. Chemie Int. Ed.*, 2019, **58**, 17651–17655.
169 M. Dong, Z. Wang, Z. Lin, Y. Zhang, Z. Chen, Y. Wu, H. Ma, Z. An, L. Gu and W. Huang, *J. Am. Chem. Soc.*, 2025, **147**, 4069–4078.
170 P. Li, Y. Yu, J. Zhou, S. Wei, J. Han, X. Li, M. Wei, T. Chen and W. Lu, *Small*, 2025, DOI:10.1002/smll.202508588.
171 J. You, C. Yin, S. Wang, X. Wang, K. Jin, Y. Wang, J. Wang, L. Liu, J. Zhang and J. Zhang, *Nat. Commun.*, 2024, **15**, 7149.
172 Z. Yang, P. Zhang, X. Chen, Z. Hong, J. Gong, X. Ou, Q. Wu, W. Li, X. Wang, L. Xie, Z. Zhang, Z. Yu, X. Qin, J. Tang, H. Zhang, Q. Chen, S. Han and H. Yang, *Adv. Mater.*, 2023, DOI:10.1002/adma.202309413.
173 T. Pan, Y. Shen, S. Zhang, W. Huang and W.-Y. Lai, *Nano Res.*, 2026, **19**, 94908248.
174 Y. Deng, P. Chen, X. Yang, N. Li, S. Ma, Z. Huang and S. Lü, *Adv. Mater.*, 2026, DOI:10.1002/adma.202514693.
175 D. Ding, X. Xu, J. Lv, F. Li, D. Liu, E. Zakhidov and M. Sun, *Dye. Pigment.*, 2026, **248**, 113534.
176 H. Gao and X. Ma, *Aggregate*, 2021, DOI:10.1002/agt2.38.
177 Q. Gao, M. Shi, Z. Lü, Q. Zhao, G. Chen, J. Bian, H. Qi, J. Ren, B. Lü and F. Peng, *Adv. Mater.*, 2023, DOI:10.1002/adma.202305126.
178 M. Cao, Y. Ren, Y. Wu, J. Shen, S. Li, Z.-Q. Yu, S. Liu, J. Li, O. J. Rojas and Z. Chen, *Nat. Commun.*, 2024, **15**, 2375.